

X-ray Diffraction

applied to the study of polycrystalline materials

Prof. Paolo Scardi

Department of Materials Engineering and
Industrial Technologies, University of Trento

These slides were used during the ICTP School on Synchrotron Radiation and Applications - Gargnano (TS), May 15th 2006. They are part of the X-ray Diffraction course for the PhD programme in Materials Engineering at the University of Trento. © All rights reserved. Do not copy - do not reproduce





PROGRAMME

Part I

- Powder Diffraction and reciprocal lattice
- Diffraction: theoretical elements

Part II

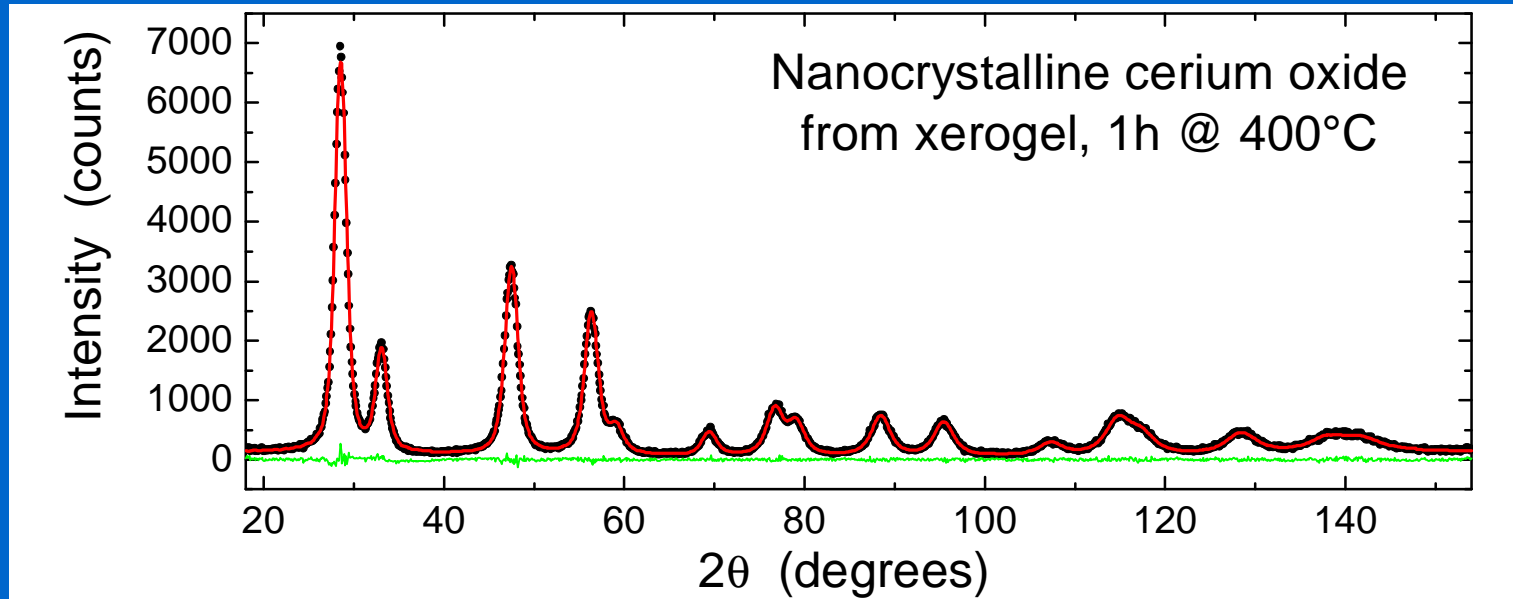
- Applications of powder diffraction:
a survey

Part III

- Introduction to line profile analysis for
the study of nanocrystalline and heavily
deformed materials



DIFFRACTION LINE BROADENING



M. Leoni, R. Di Maggio, S. Polizzi & P. Scardi, *J. Am. Ceram. Soc.* 87 (2004) 1133.

What information can be obtained on
nanocrystalline and heavily deformed materials ?

What is the origin of the
Line Broadening effect?



Most common sources of line broadening

- crystalline domain size and shape (and distribution)
- generalised line defects, e.g., dislocations, disclinations
- planar faults, e.g., twin and deformation faults
- anti-phase domain boundaries (in ordered phases)
- residual (micro)strain (e.g. by misfitting inclusions)
- grain surface effects (e.g. grain surface relaxation)
- lattice parameter fluctuation from grain to grain (e.g. impurities)
-

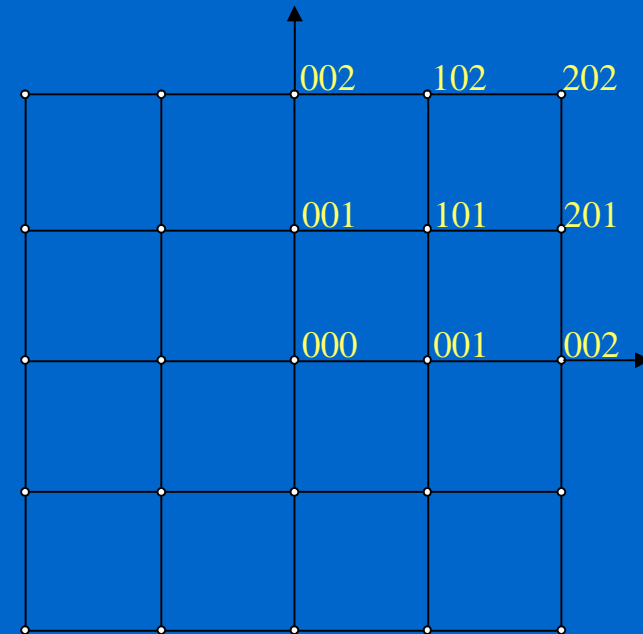
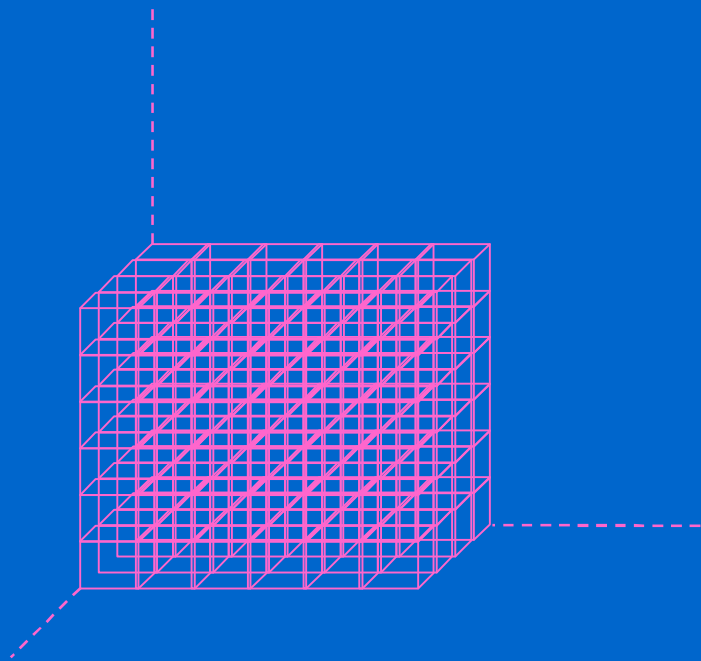


Origin of diffraction line broadening



DOMAIN SIZE EFFECT

The reciprocal space is made of points (representing families of hkl planes). Formally this is true only for *perfect* crystals, i.e., infinite crystals with no defects (e.g. no surface) to interrupt the coherency of the crystalline lattice

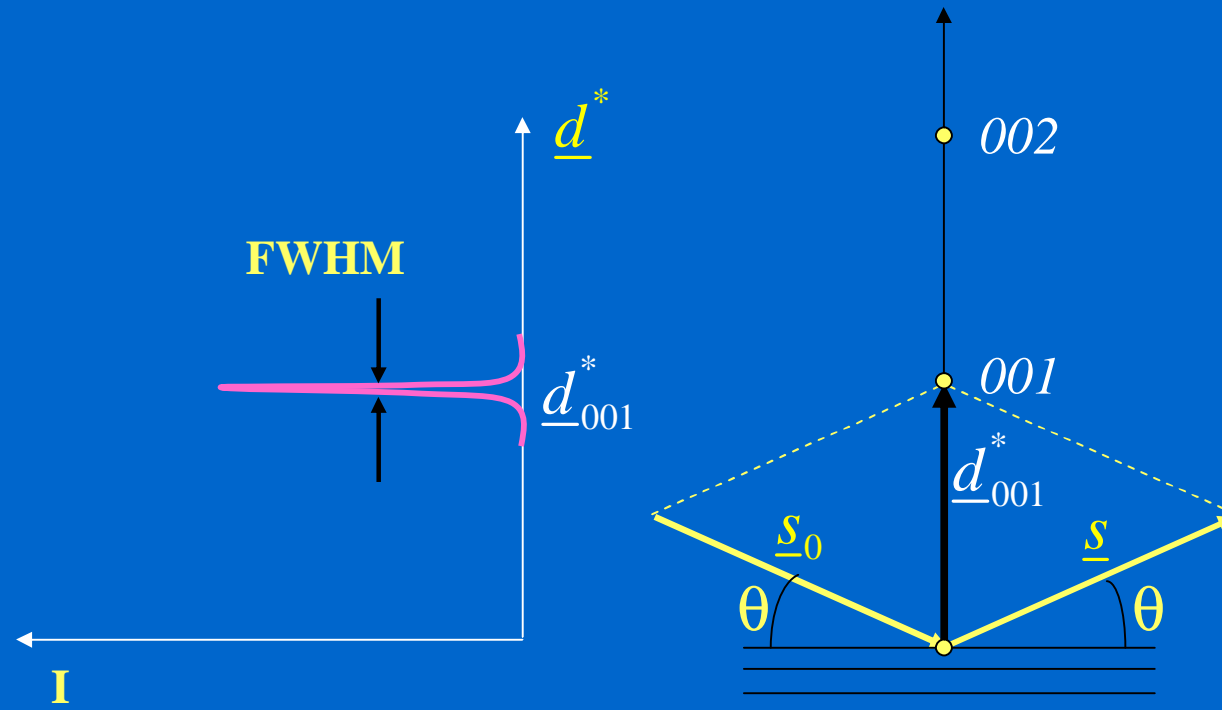




DOMAIN SIZE EFFECT

For a *perfect (infinite)* crystal, peak width is determined only by the instrumental resolution

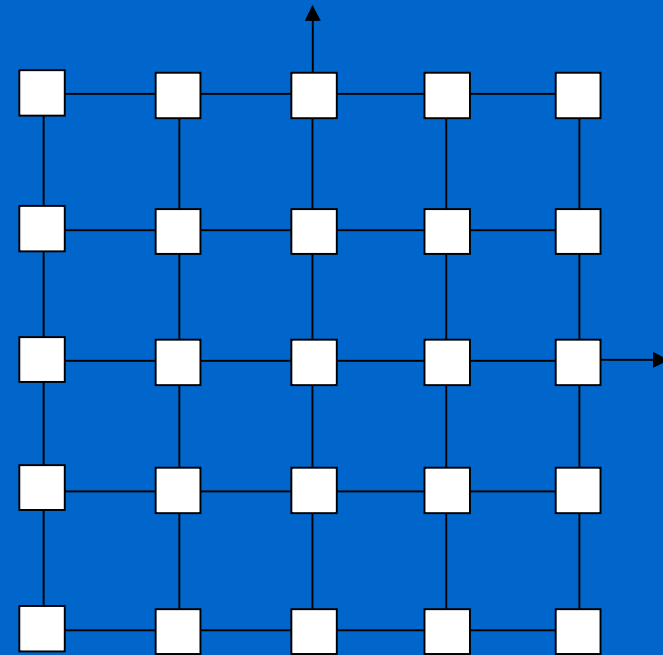
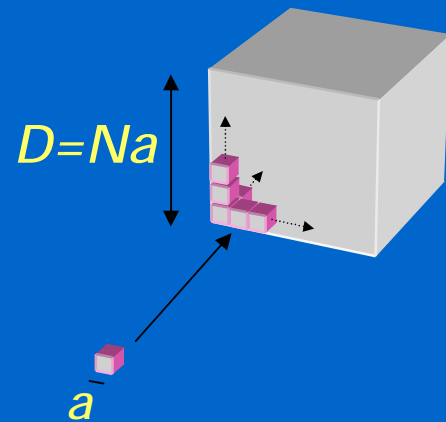
$$|\underline{s} - \underline{s}_0| = \frac{2 \sin \varphi}{l} = \frac{1}{d_{hkl}} = d_{hkl}^*$$





DOMAIN SIZE EFFECT

For a *finite crystal* ($D < 1\text{mm}$) point size is finite (measurable), and it increases by decreasing the crystalline domain size





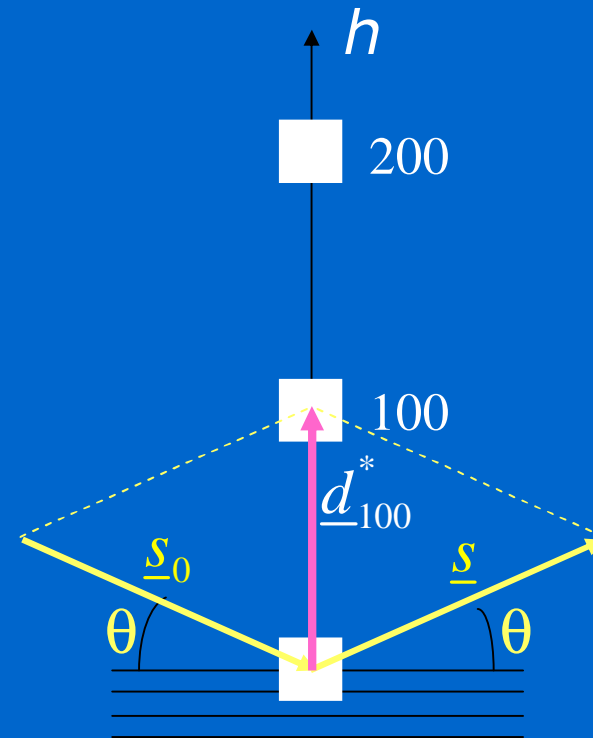
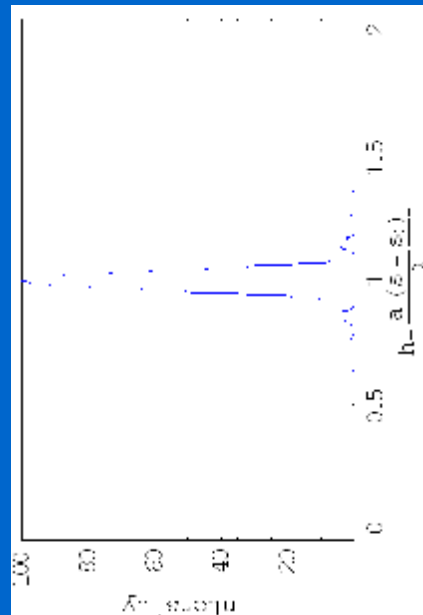
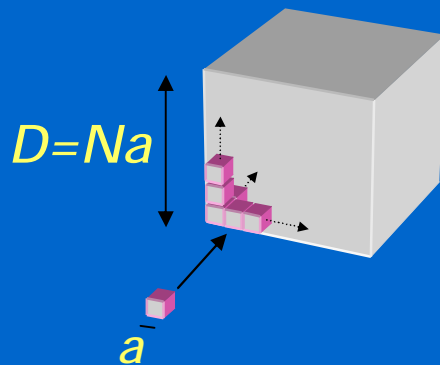
DOMAIN SIZE EFFECT

Point shape is related (reciprocal) to the shape of the crystallite. The intensity varies across the point, and for a cubic crystal it follows the trend of the *interference function*:

$$I \propto |F_T|^2 \frac{\sin^2(pNh)}{(ph)^2} \frac{\sin^2(pNk)}{(pk)^2} \frac{\sin^2(pNl)}{(pl)^2}$$

Along the [h00] direction:

$$I \propto \frac{\sin^2(pNh)}{(ph)^2}$$

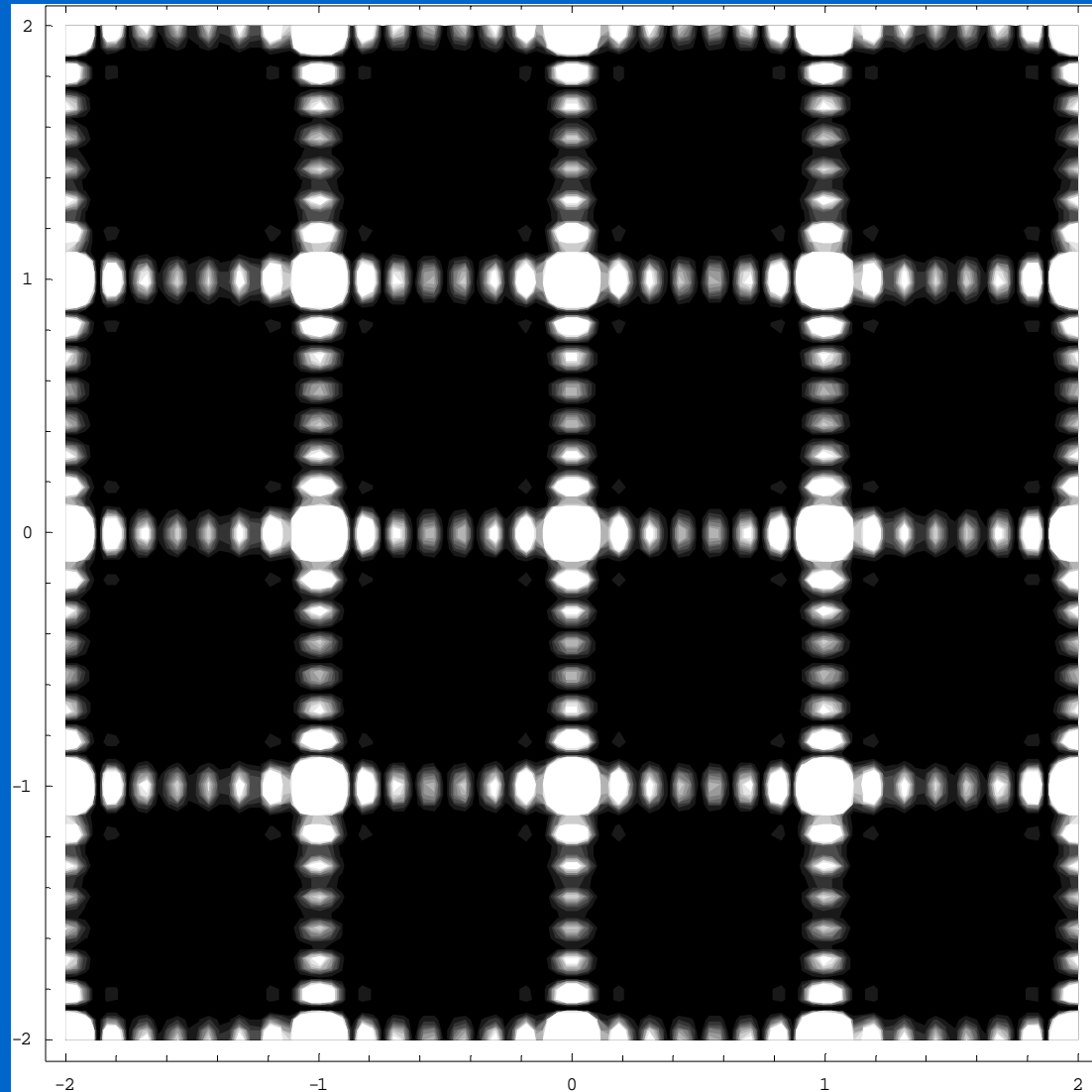




DOMAIN SIZE EFFECT

For $hk0$ lines, $N=8$:

$$I \propto |F_T|^2 \frac{\sin^2(pNh)}{(ph)^2} \frac{\sin^2(pNk)}{(pk)^2}$$



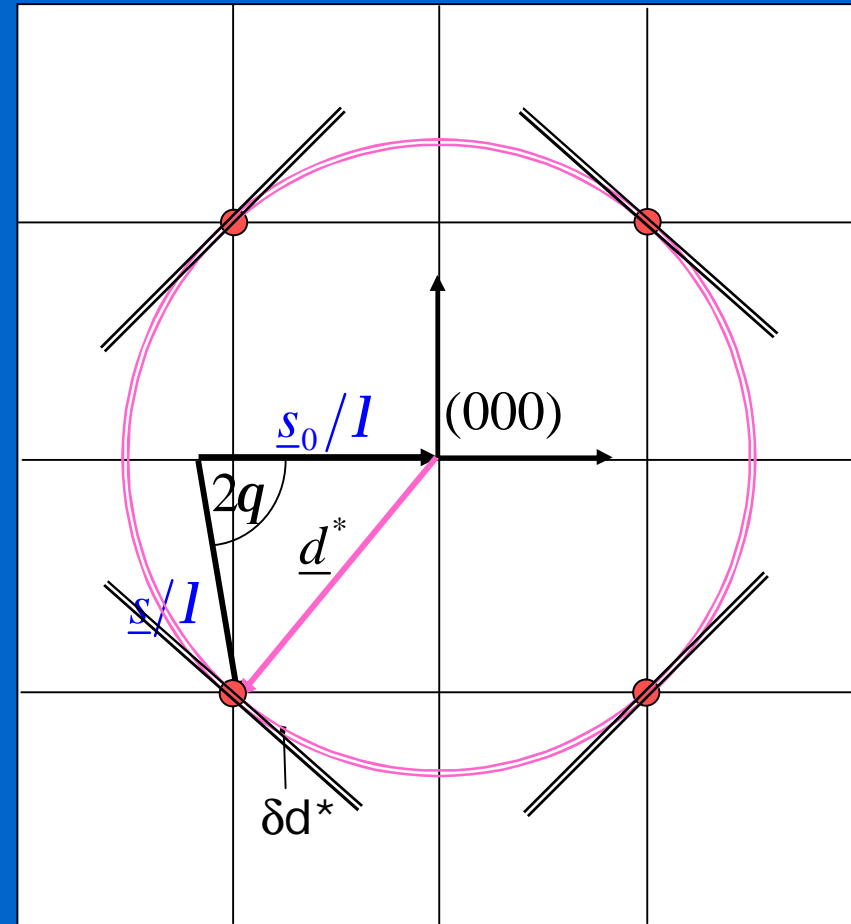
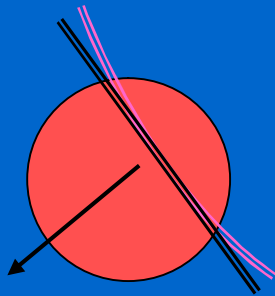


DOMAIN SIZE EFFECT IN POWDER DIFFRACTION

When approaching the Bragg condition the sphere starts crossing the points.

The intensity measured between q and $q+dq$ is proportional to the intensity between d^* and d^*+dd^*

Point spreads over a region much smaller than d^* : integration over the spherical surfaces can be replaced by integration over tangent planes

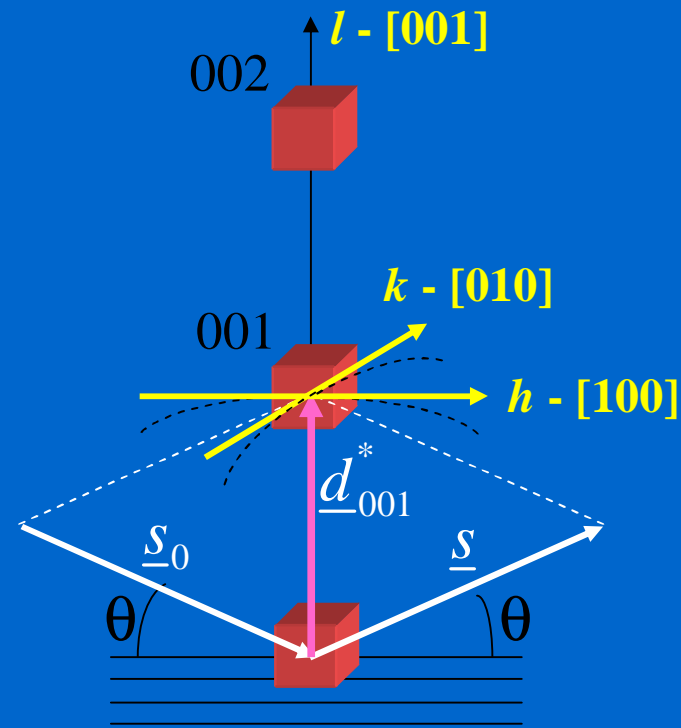
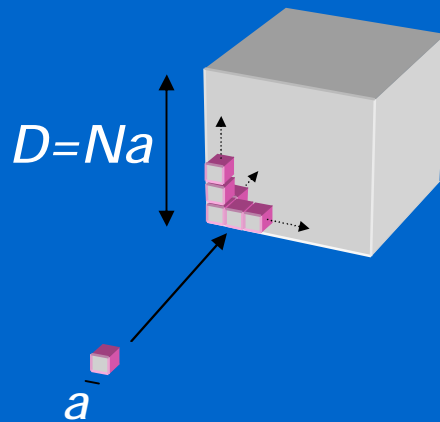




DOMAIN SIZE EFFECT IN POWDER DIFFRACTION

The peak profile in a powder pattern is given by the integral of the intensity in the reciprocal space over the sphere of radius d^* (approximated by the tangent plane).

The integration depends on: (a) *shape* of the 'point' (i.e., of the crystallite) and (b) *direction* along which the point is crossed (related to the Miller indices for the given peak).



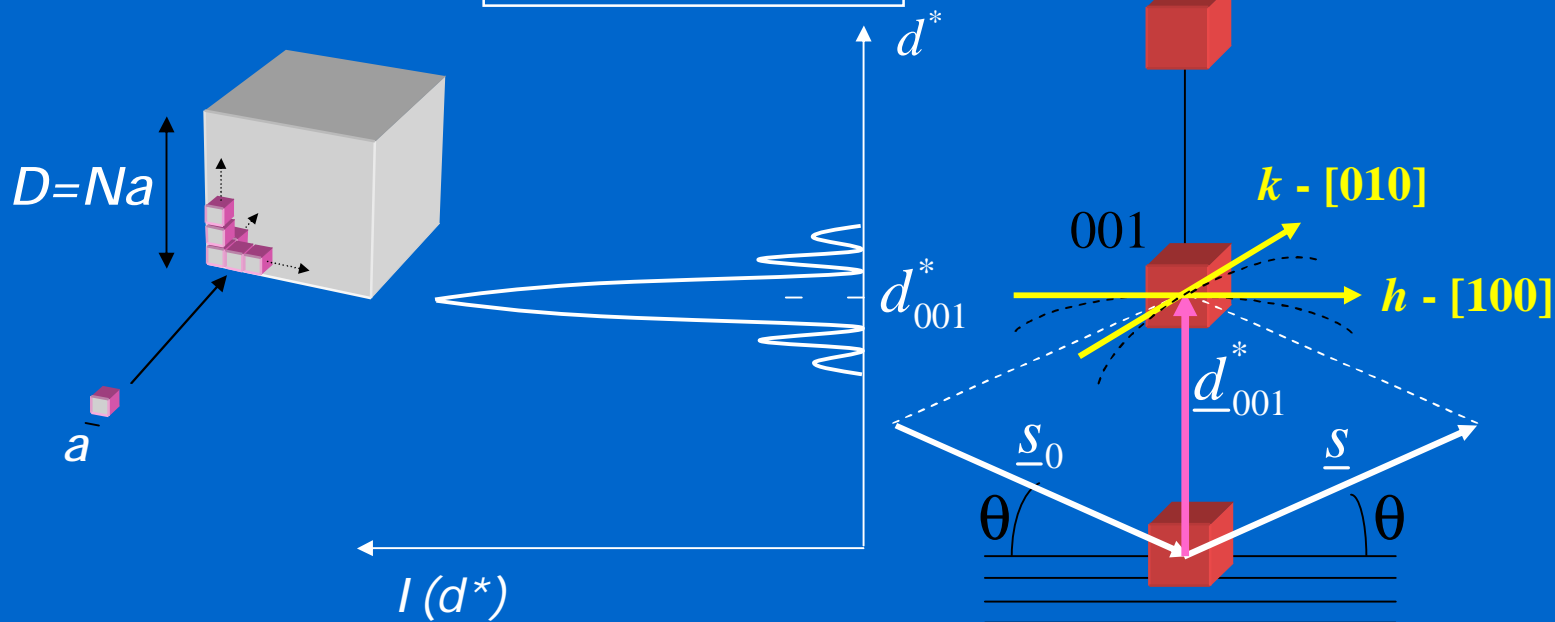


DOMAIN SIZE EFFECT IN POWDER DIFFRACTION

In the simple case shown below ((001) peak, cubic crystallite, edge D)

$$I \propto |F_T|^2 \iint \frac{\sin^2(pNh)}{(ph)^2} \frac{\sin^2(pNk)}{(pk)^2} \frac{\sin^2(pNl)}{(pl)^2} dh \cdot dk \rightarrow |F_T|^2 \frac{\sin^2(pNl)}{(pl)^2}$$

$$l = \underline{a} \cdot \frac{\underline{s} - \underline{s}_0}{l} = \underline{a} \cdot \underline{d}^* \Rightarrow \boxed{I(d^*) \propto \frac{\sin^2(pNad^*)}{(pad^*)^2}}$$

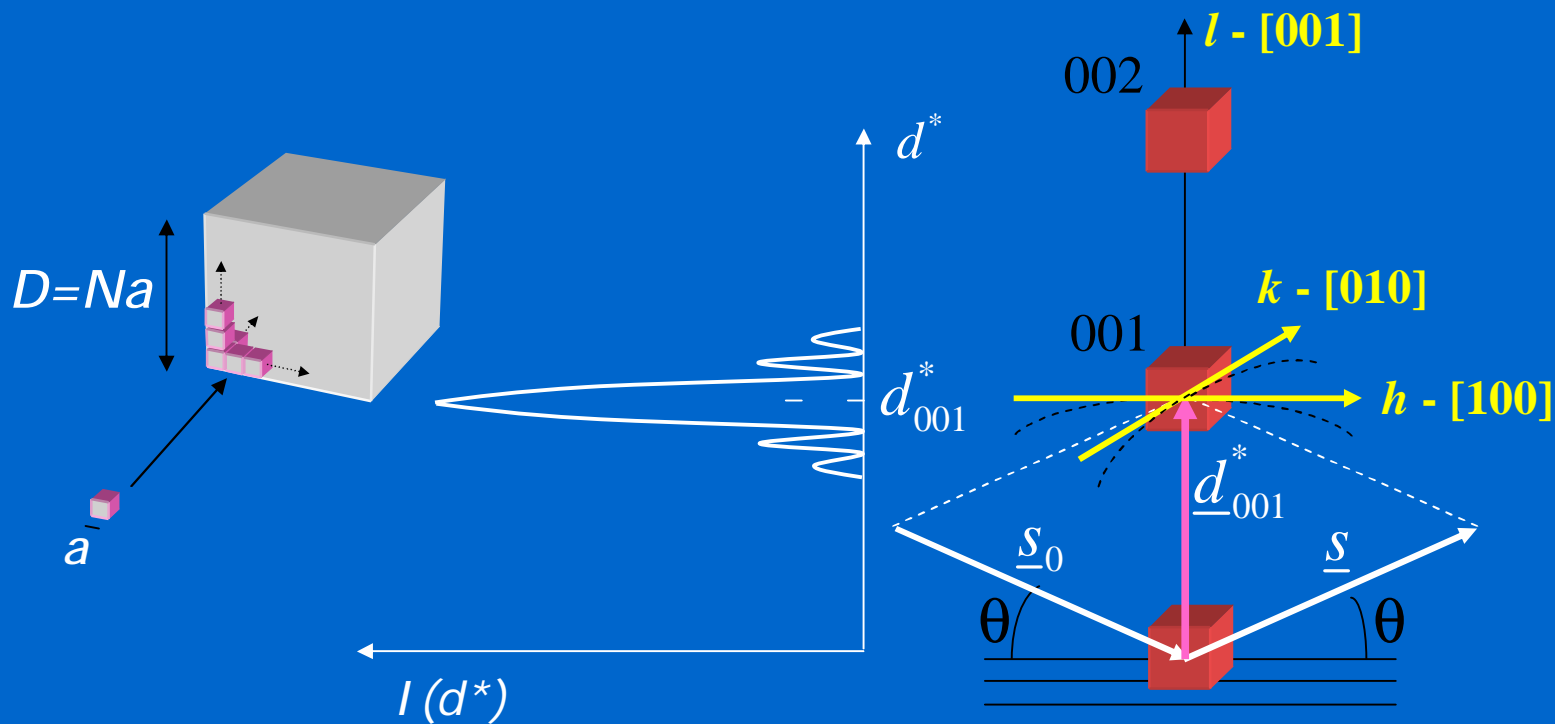




DOMAIN SIZE EFFECT IN POWDER DIFFRACTION

Exploiting the properties of $\frac{\sin^2(pNad^*)}{(pad^*)^2}$, the integral breadth is given by:

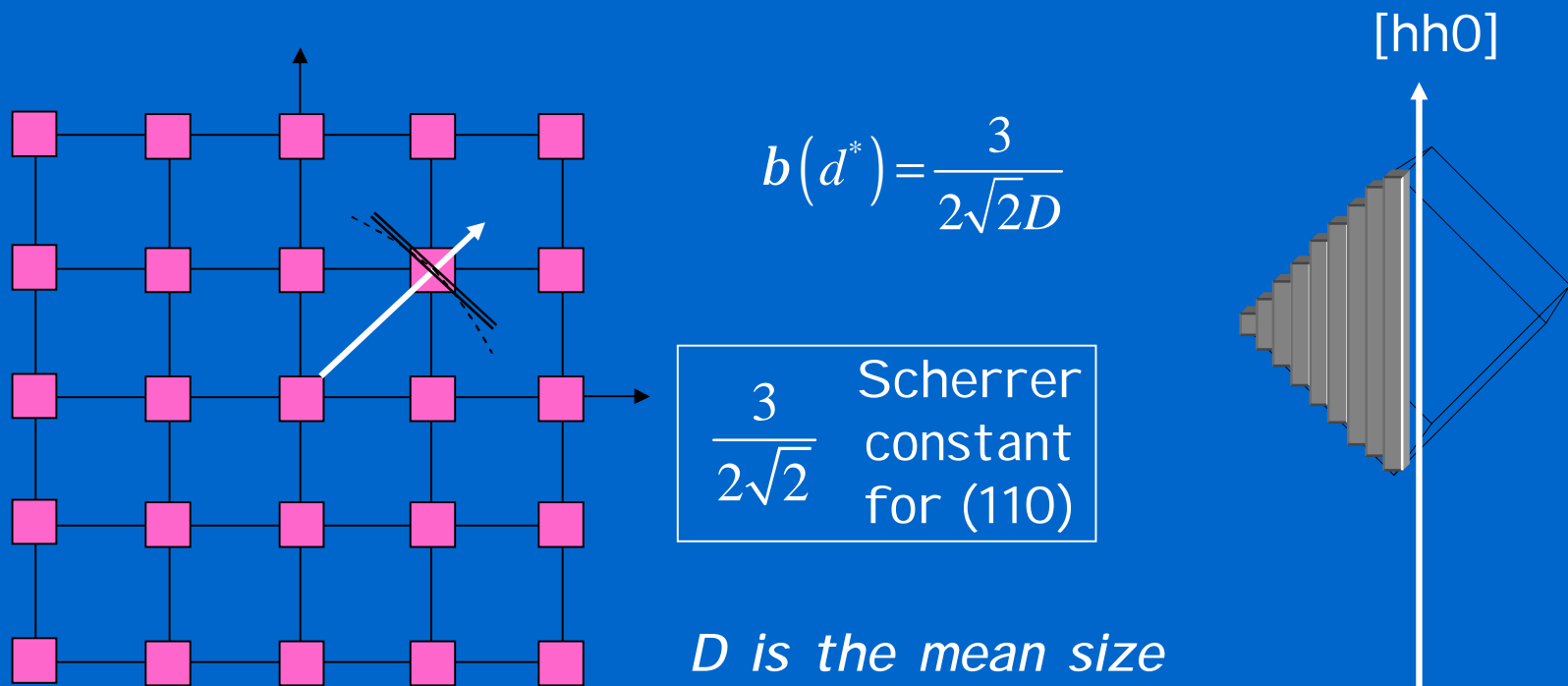
$$b(d^*) = \frac{\text{Peak Area}}{\text{Peak Maximum}} = \frac{\int_{-\infty}^{\infty} \frac{\sin^2(pNad^*)}{(pad^*)^2} dd^*}{I(0)} = \frac{1}{Na} = \frac{1}{D} \leftarrow \text{Scherrer formula}$$





DOMAIN SIZE EFFECT IN POWDER DIFFRACTION

For any other crystallite shape and (hkl) reflections the result is different. The interlattice breadth is in any case inversely proportional to the domain size, but a geometrical coefficient (*Scherrer constant*) must be calculated for each specific case.





DOMAIN SIZE EFFECT IN POWDER DIFFRACTION

For a powder made of spherical crystallites of diameter D , the Scherrer constant is the same for any (hkl):

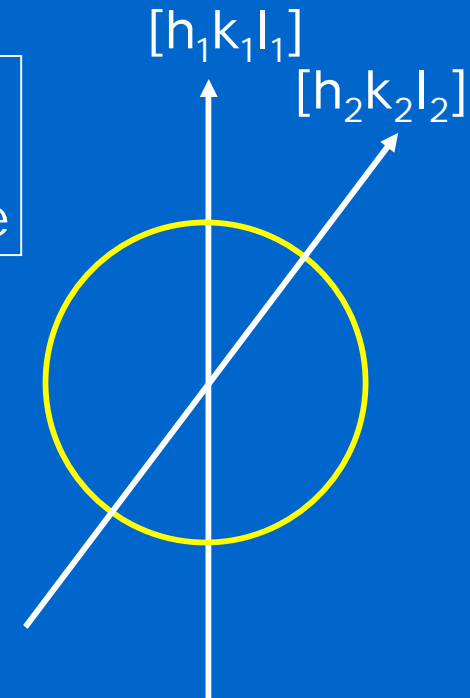
$$b(d^*) = \frac{4}{3D}$$

$\frac{4}{3}$	Scherrer constant for sphere
---------------	------------------------------

In general, for crystallites with simple shapes (convex solids like spheres, cubes, octahedra, tetrahedra, ...)

$$b(d^*) = \frac{K_b}{D}$$

where K_b is the Scherrer constant (for the integral breadth), different for the various crystallite shapes and for different (hkl)



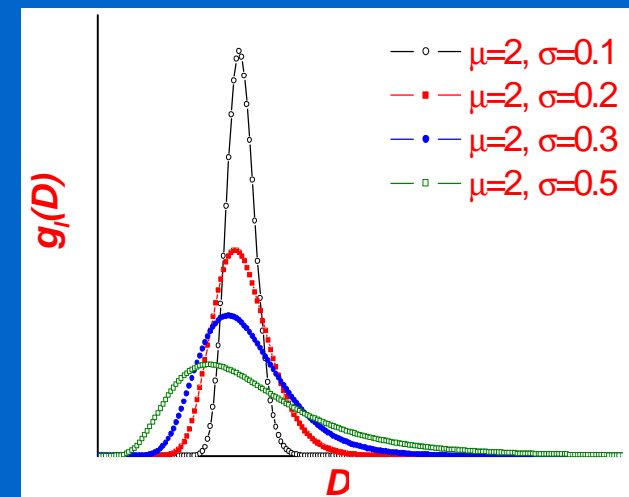


DOMAIN SIZE BROADENING

If the powder is made of a *distribution* $g(D)$ of crystallites (with same shape) of volume $V_c(D)$, the diffracted profile is a weighted average of the intensity from a single crystallite (I_c):

$$I(d^*) = k(d^*) \frac{\int_0^{\infty} I_c(d^*, D) g(D) V_c(D) dD}{\int_0^{\infty} g(D) V_c(D) dD}$$

e.g., lognormal distributions à



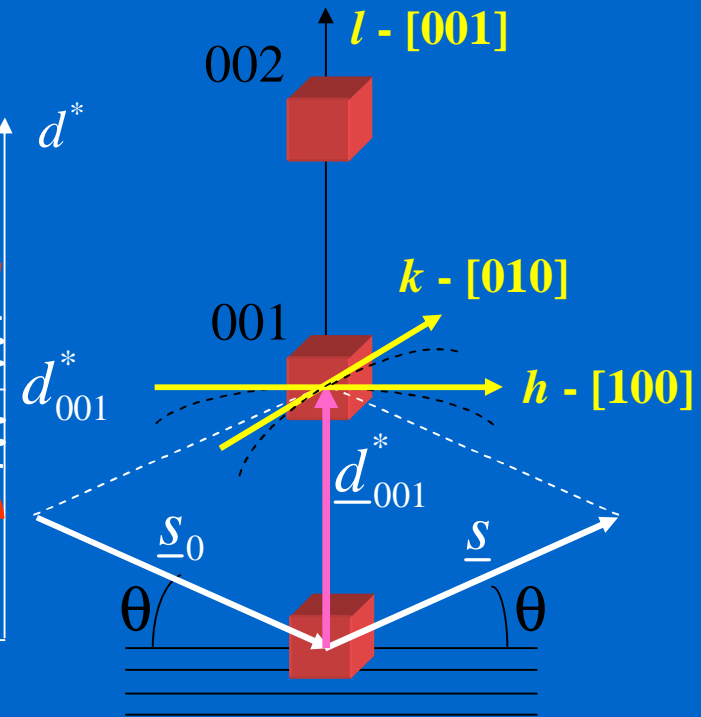


DOMAIN SIZE EFFECT IN POWDER DIFFRACTION

As a consequence, features of the profile of a single crystallite are 'embedded' in the overall profile for the dispersed system.

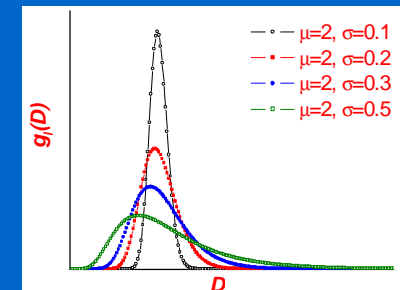
$$b(d_{hkl}^*) = K_b \frac{M_3}{M_4} = \frac{K_b}{\langle D \rangle}$$

$I(d^*)$



If a size distribution is present (polydisperse system), the integral breadth gives an average size $\langle D \rangle$ given by:

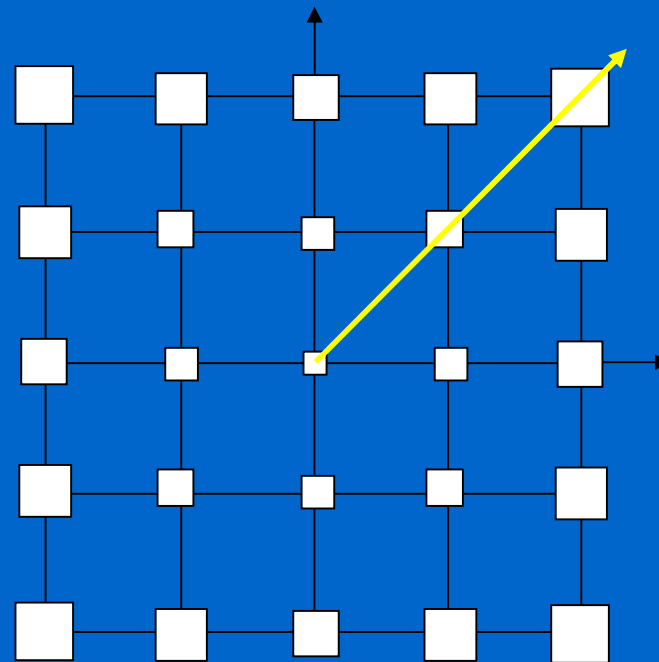
where M_3 and M_4 are the 3rd and 4th moments of $g(D)$





MICROSTRAIN EFFECT IN POWDER DIFFRACTION

The distortion effect of lattice defects (dislocations, faulting, inclusions, etc), is quite complex. The effect of a lattice deformation can modify both the position and the width and shape of the reciprocal space points. Differently from the 'size' effect, the 'strain' effect *depends on d^**





MACROSTRAIN EFFECT

By using an heuristic approach, differentiating the Bragg law (with $\lambda = \text{constant}$) one can demonstrate that

$$0 = 2\Delta d \sin(q) + 2d \cos(q) \Delta(q)$$

Introducing the strain: $e = \Delta d/d$

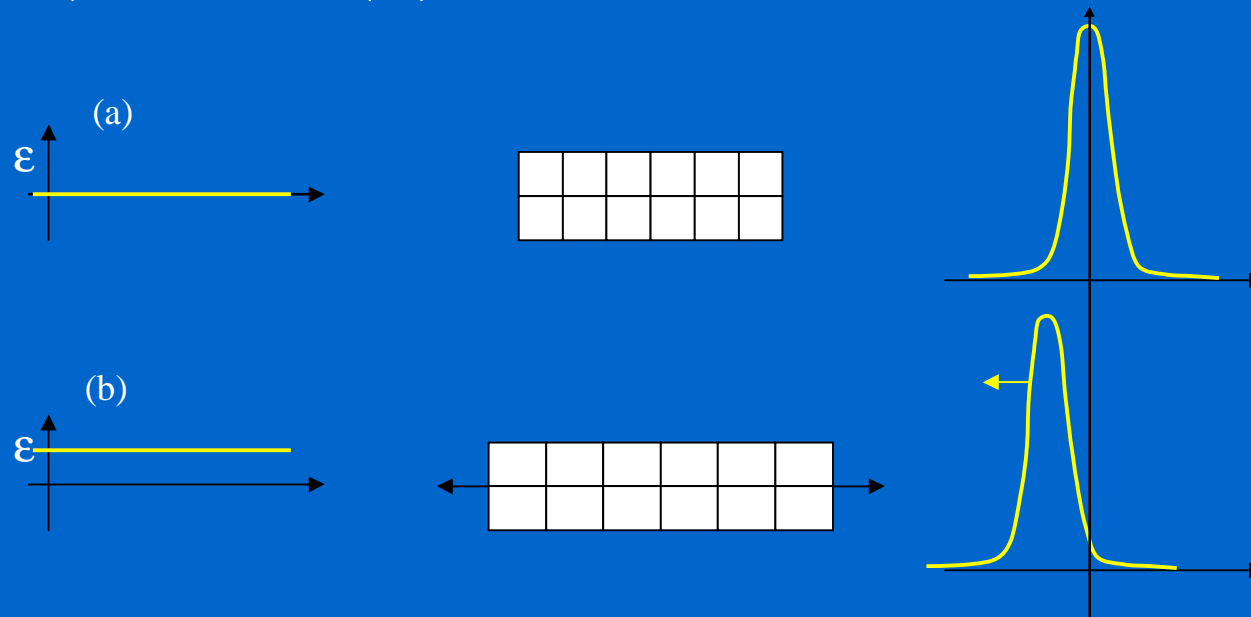
$$\Delta(2q) = -2 \tan(q) \frac{\Delta d}{d} = -2e \tan(q)$$



MACROSTRAIN EFFECT

The presence of a uniform strain, produces a *shift* in the position of the diffraction peaks \implies *Residual strain/stress analysis*

$$\Delta(2q) = -2e \tan(q)$$

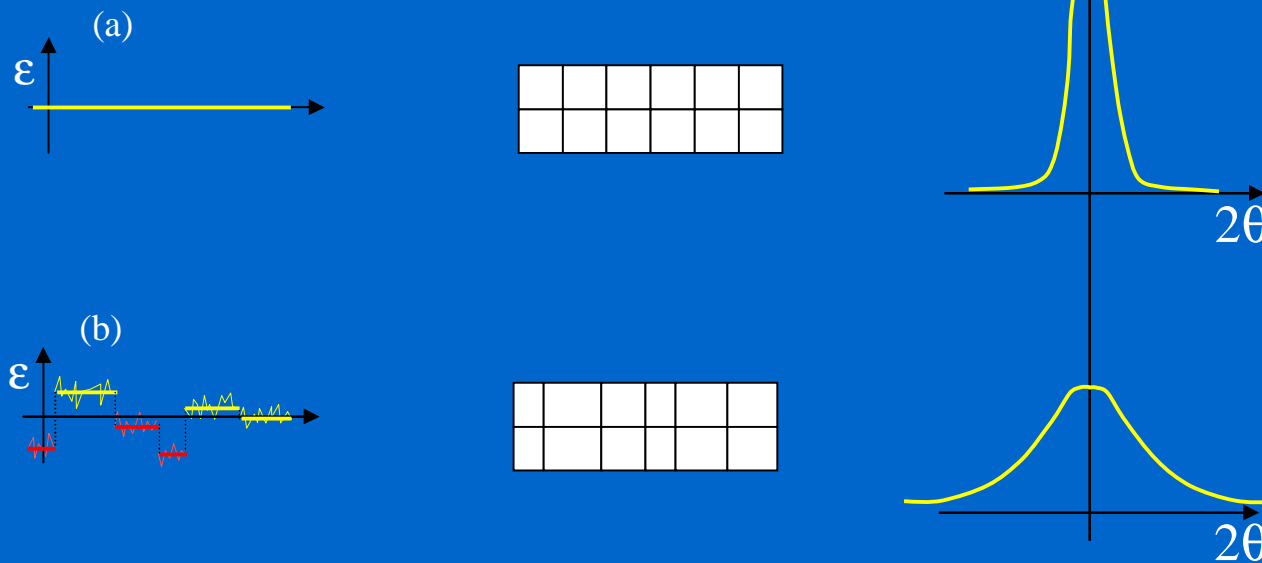




MICROSTRAIN EFFECT IN POWDER DIFFRACTION

If a non-uniform strain is present, then a microstrain (r.m.s. strain) must be considered $\langle e^2 \rangle^{1/2} = \langle (\Delta d/d)^2 \rangle^{1/2}$, which is related to a strain distribution $p_L(e)$ (whose mean can also be zero)

$$b(2q) \approx 2 \langle e^2 \rangle^{1/2} \tan q$$

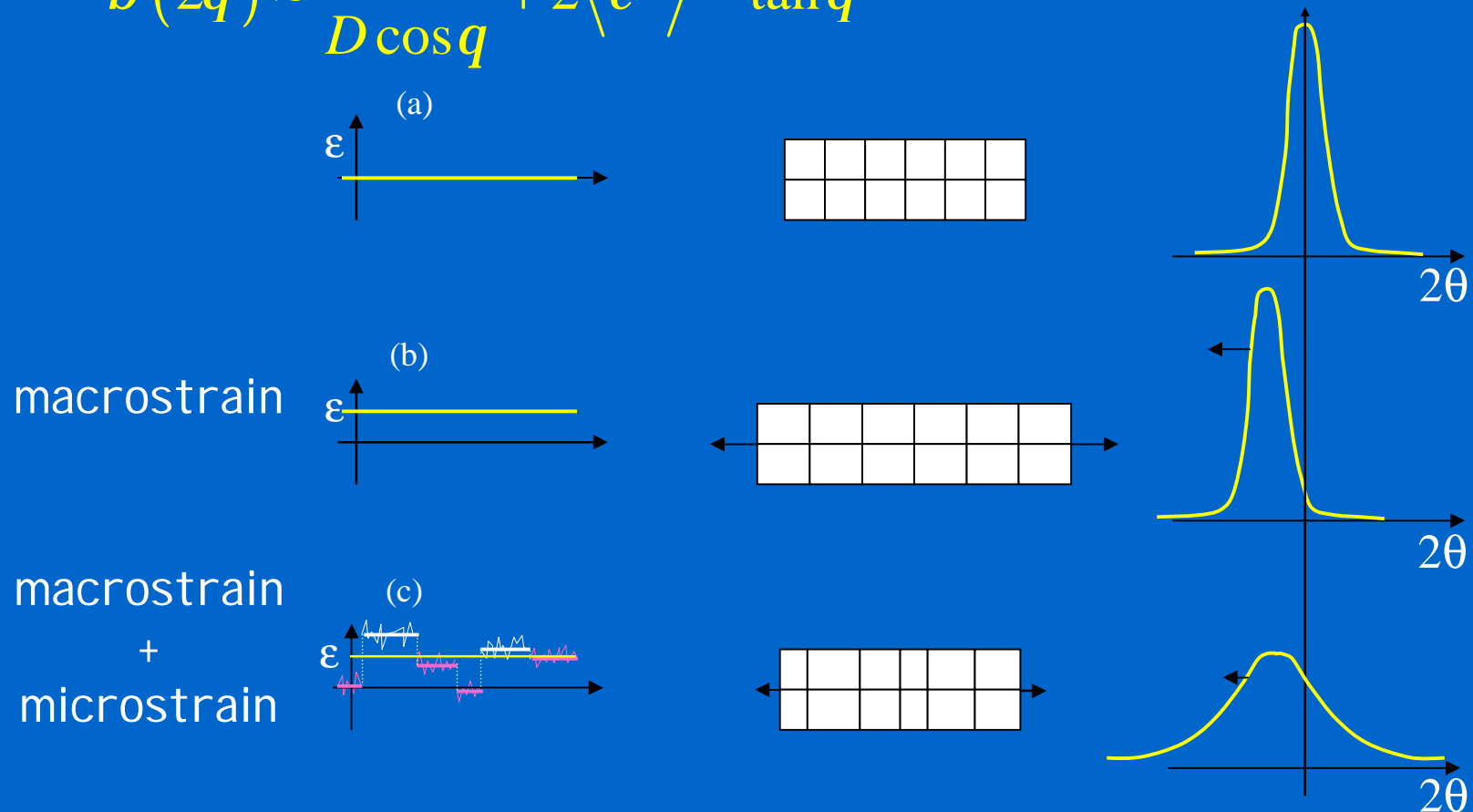




COMBINED 'SIZE-STRAIN' EFFECT

If the combined effect is considered – domain size and lattice distortions – then one can write (as a first order approximation):

$$b(2q) \approx \frac{Kl}{D \cos q} + 2 \langle e^2 \rangle^{1/2} \tan q$$



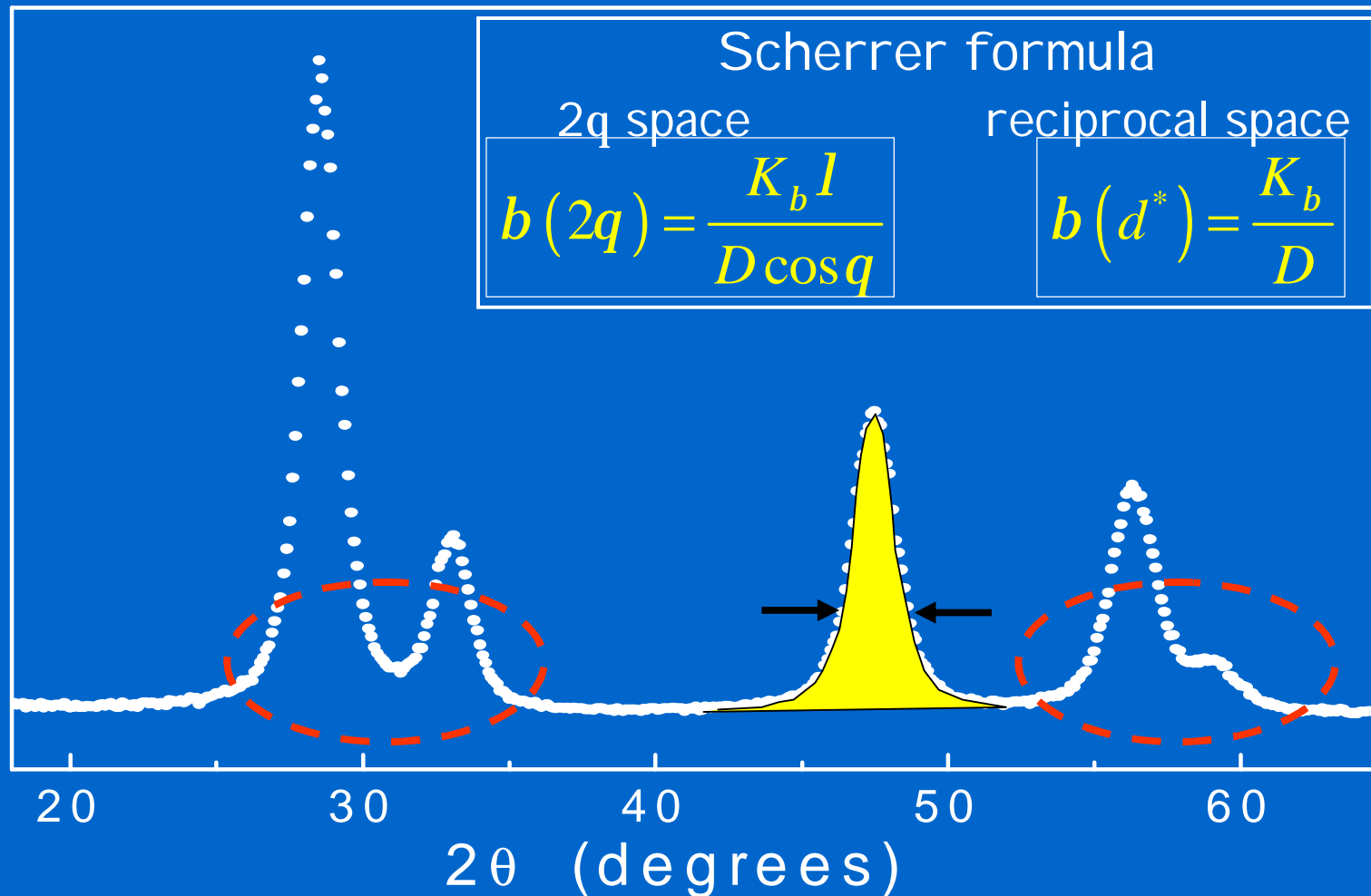


Traditional methods of line profile analysis



INTEGRAL BREADTH METHODS

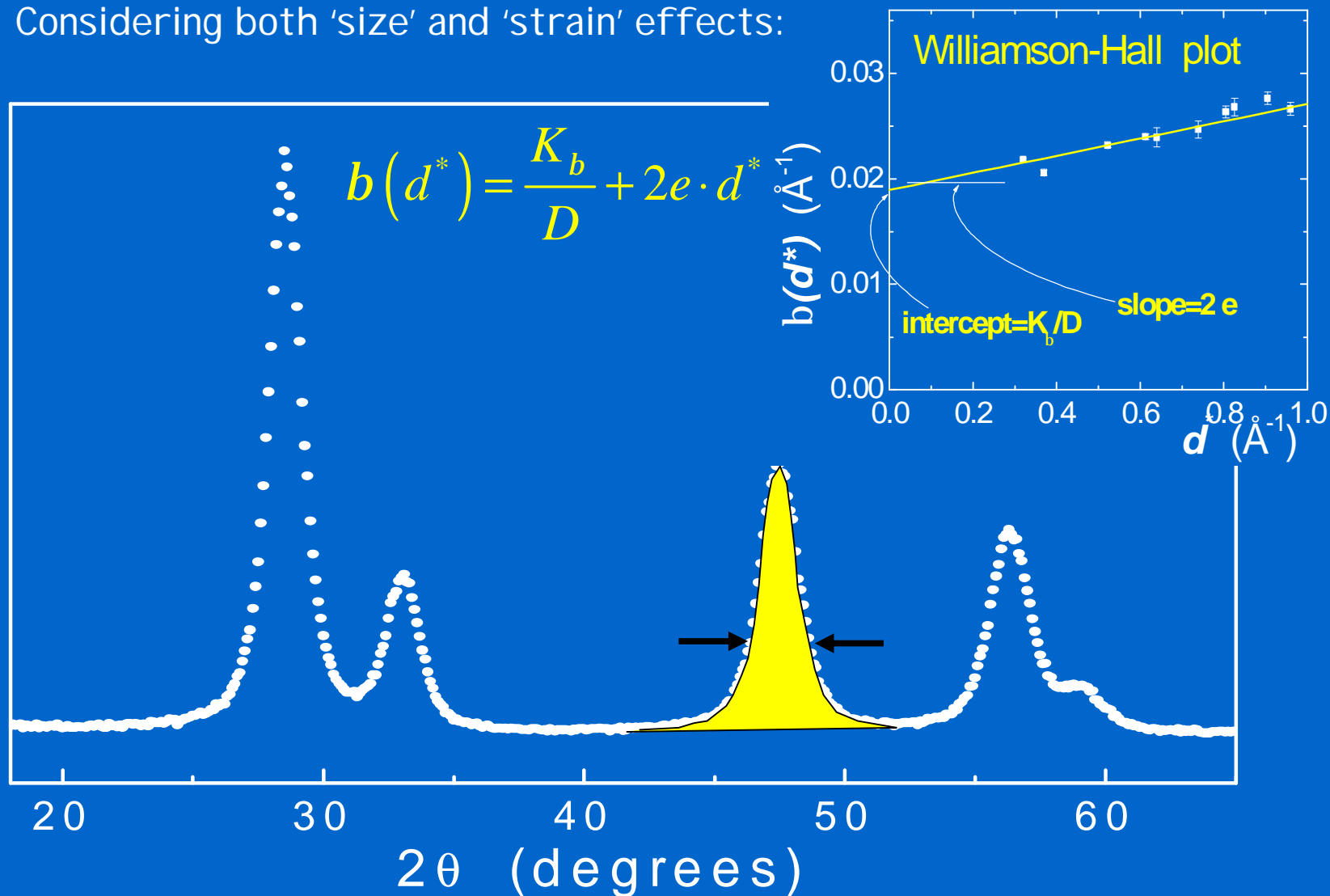
Line profile information can be represented by the **integral breadth** (β =peak area/peak maximum). If only 'size' effects are considered, then:





INTEGRAL BREADTH METHODS

Considering both 'size' and 'strain' effects:

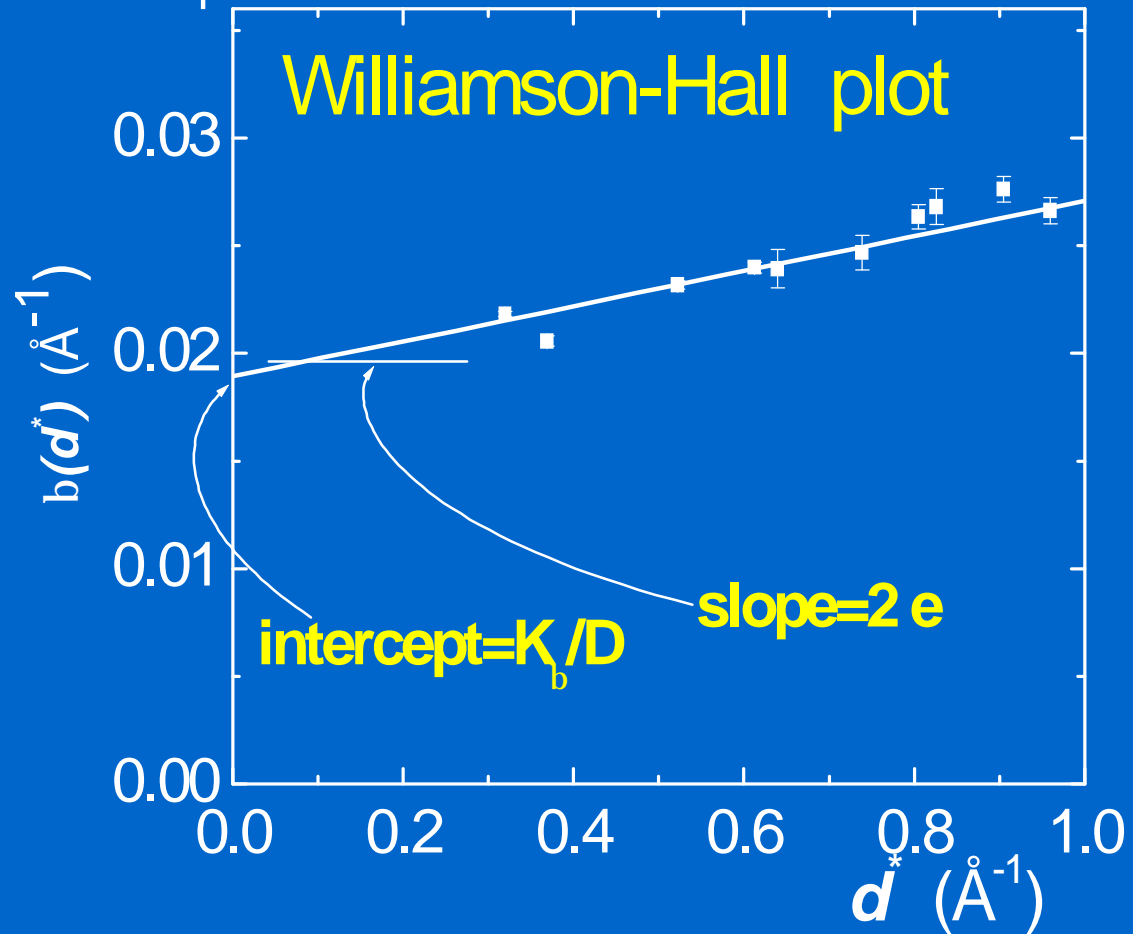




INTEGRAL BREADTH METHODS

The method is simple and easy to apply, even if it is based on quite simplified hypotheses (e.g., the additivity of the two terms). Results are mostly to be considered as qualitative.

$$b(d^*) = \frac{K_b}{D} + 2e \cdot d^*$$





FOURIER METHODS

The PD profile is a convolution (\otimes) of profile components produced by different sources: instrumental profile (IP), domain size (S), microstrain (D), faulting (F), anti-phase domain boundaries (APB), stoichiometry fluctuations (C), grain surface relaxation (GSR), etc.

$$I(d^*) = I^{IP}(d^*) \otimes I^S(d^*) \otimes I^D(d^*) \otimes I^F(d^*) \otimes I^{APB}(d^*) \otimes I^C(d^*) \otimes I^{GRS}(d^*) \dots$$

Contributions can be separated by means of a FOURIER ANALYSIS:

the Fourier Transform (FT) of $I(d^*)$ is the product of the FTs of the single profile components

Traditional Fourier methods (e.g. Warren-Averbach): (a) background subtraction and deconvolution of the instrumental component; (b) analysis of single peak profiles



WARREN-AVERBACH METHOD

After the background has been subtracted and the instrumental profile (IP) component deconvoluted, the Fourier Transform of the diffraction peak profile is:

$$I(d^*) = k(d^*) \int A_L e^{2\pi i L d^*} dL$$



Fourier coefficients $A_L = A_L^S \cdot A_L^D$
for size (S) and strain (D) effects

$$(L = n d_{hkl})$$

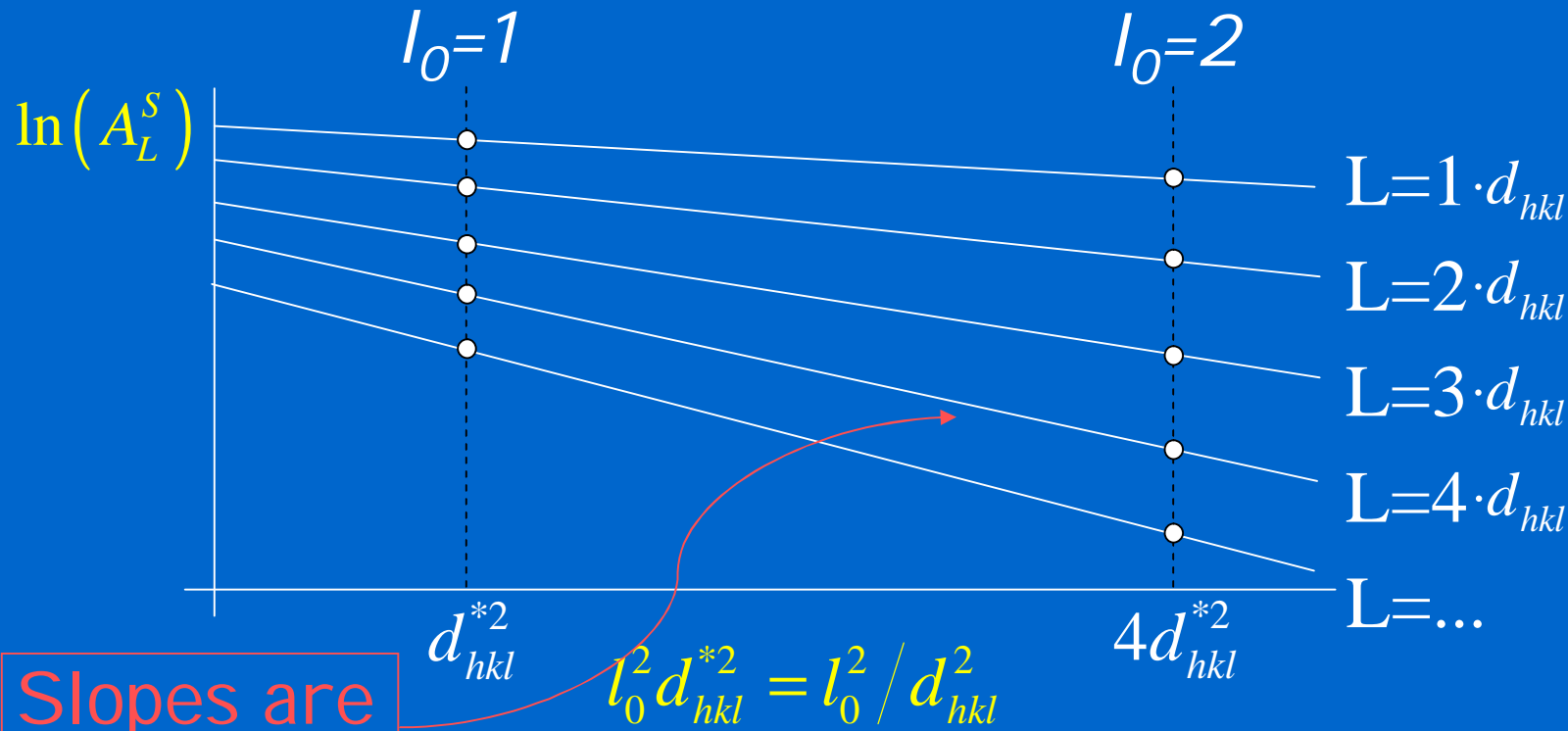
According to the Warren-Averbach method (l_0 is the diffraction order):

$$\ln(A_L) ; \ln(A_L^S) - 2p^2 L^2 \langle e_{hkl}^2(L) \rangle l_0^2 / d_{hkl}^2$$

'Size' and 'strain terms can be separated by means of a plot of $\ln(A_L)$ as a function of $l_0^2 d_{hkl}^{*2} = l_0^2 / d_{hkl}^2$, for different values of L.



WARREN-AVERBACH METHOD



Slopes are
 $\propto \langle e_{hkl}^2(L) \rangle$

$$l_0^2 d_{hkl}^{*2} = l_0^2 / d_{hkl}^2$$

$$\ln(A_L) ; \ln(A_L^S) - 2p^2 L^2 \langle e_{hkl}^2(L) \rangle l_0^2 / d_{hkl}^2$$

Plot $\ln(A_L)$ as a function of $l_0^2 d_{hkl}^{*2} = l_0^2 / d_{hkl}^2$, for different values of L .

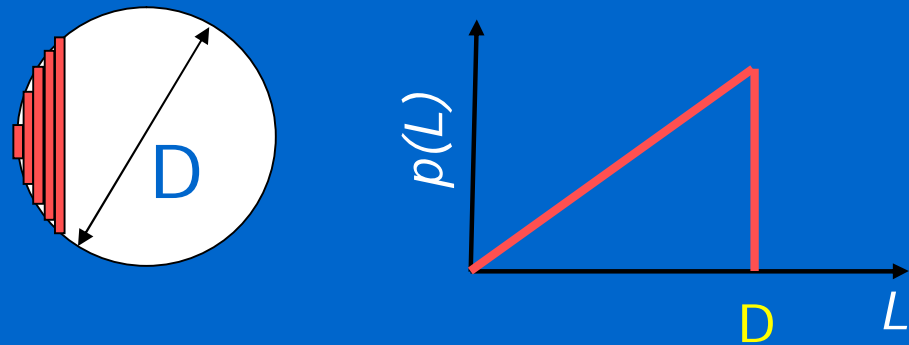


WARREN-AVERBACH METHOD

Provided that the procedure has been carried out properly (calculate Fourier Coefficients, account for background, instrumental component and peak overlapping, presence of faulting, other defects, etc.) ...

- **Size Fourier coefficients:** A_L^S
(to be related to the column length distribution, $p(L) \propto d^2 A_L^S / dL^2$)

For example, for a spherical crystallite:



- **Microstrain:** $\langle e_{hkl}^2(L) \rangle$
(to be related to the strain distribution $p(e_{hkl}(L))$ generated by the specific source of lattice strain)

... interpretation of W-A results is not straightforward



PROFILE FITTING AND LINE PROFILE ANALYSIS

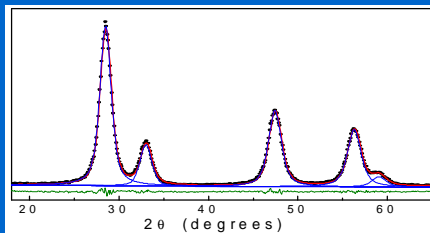
Traditional methods are generally grouped as:

- 'Simplified' methods based on the integral breadth (e.g., *Scherrer* formula, *Williamson-Hall* plot)
- **Fourier Methods** (e.g., *Warren-Averbach* method)

The practical application of these methods requires the extraction of profile data from the experimental pattern. To this purpose it is nowadays a common practice to use:



Pattern decomposition + Line Profile Analysis

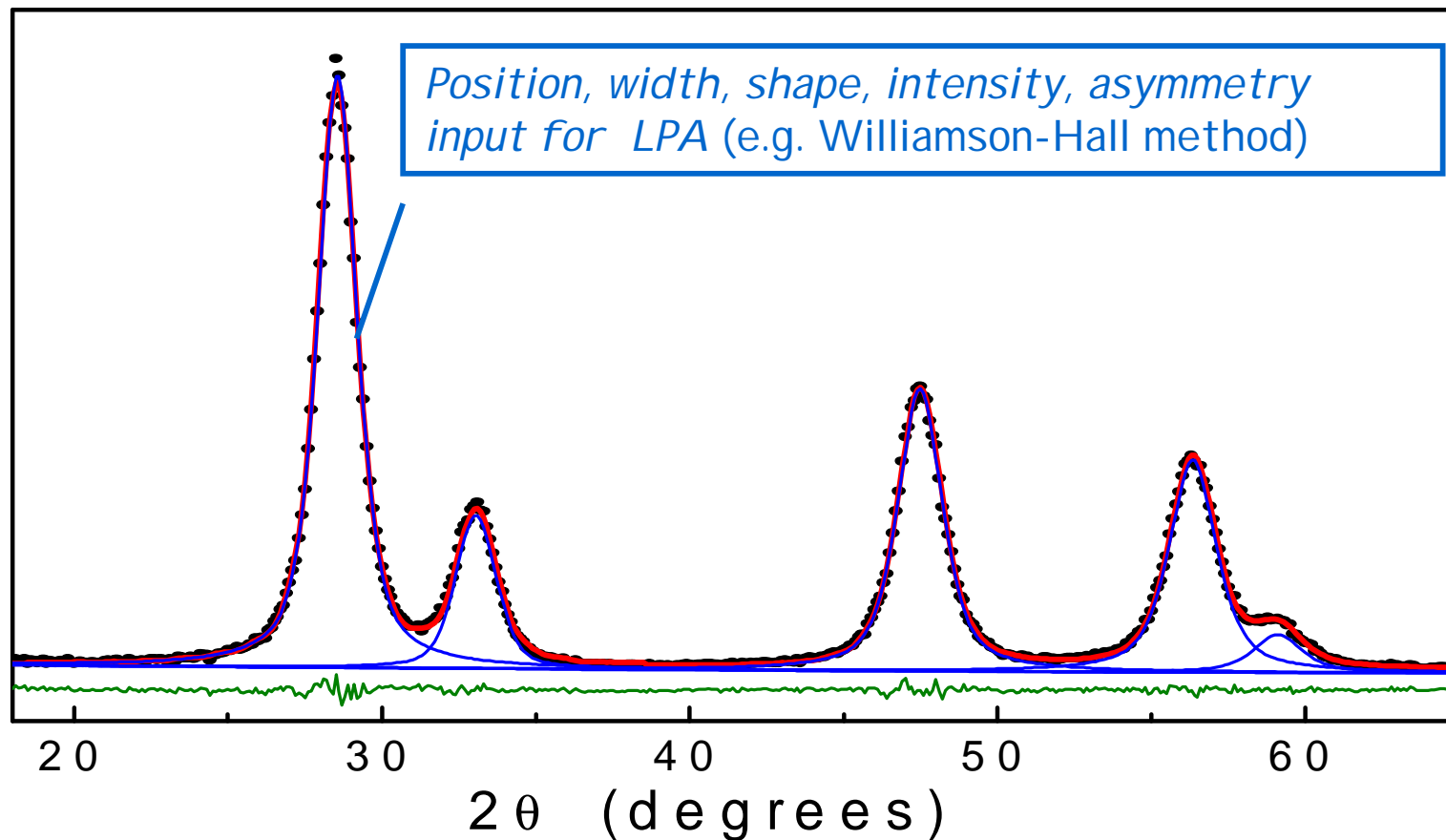


Scherrer formula, *WH* plot,
Warren-Averbach method



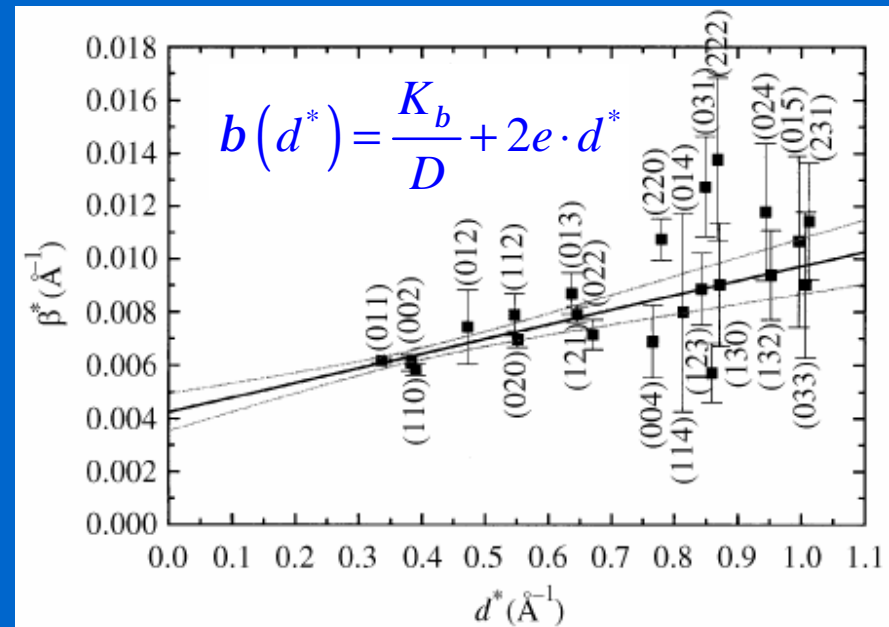
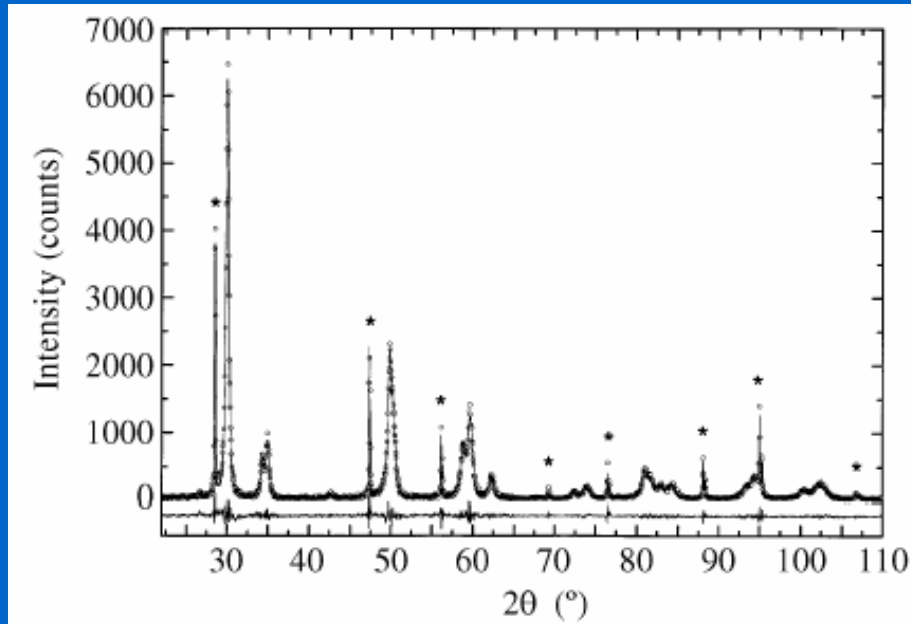
PROFILE FITTING AND LINE PROFILE ANALYSIS

Pattern decomposition by profile fitting (e.g. by MarqX) is used to extract peak profile parameters. The method employs analytical profile functions (e.g., Voigt, pV, PVII). It is a practical and flexible approach, even if it is arbitrary in that it imposes an a-priori shape to the profiles.





PROFILE FITTING + WILLIAMSON-HALL METHOD

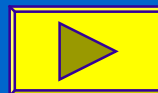


Ceria-stabilized zirconia with 20% standard Silicon (SRM 640b).

Whole Powder Pattern Fitting (WPPF) by *MarqX*.

Williamson-Hall analysis results: 1/intercept \hat{a} D~230 Å,
slope \hat{a} e~0.0027

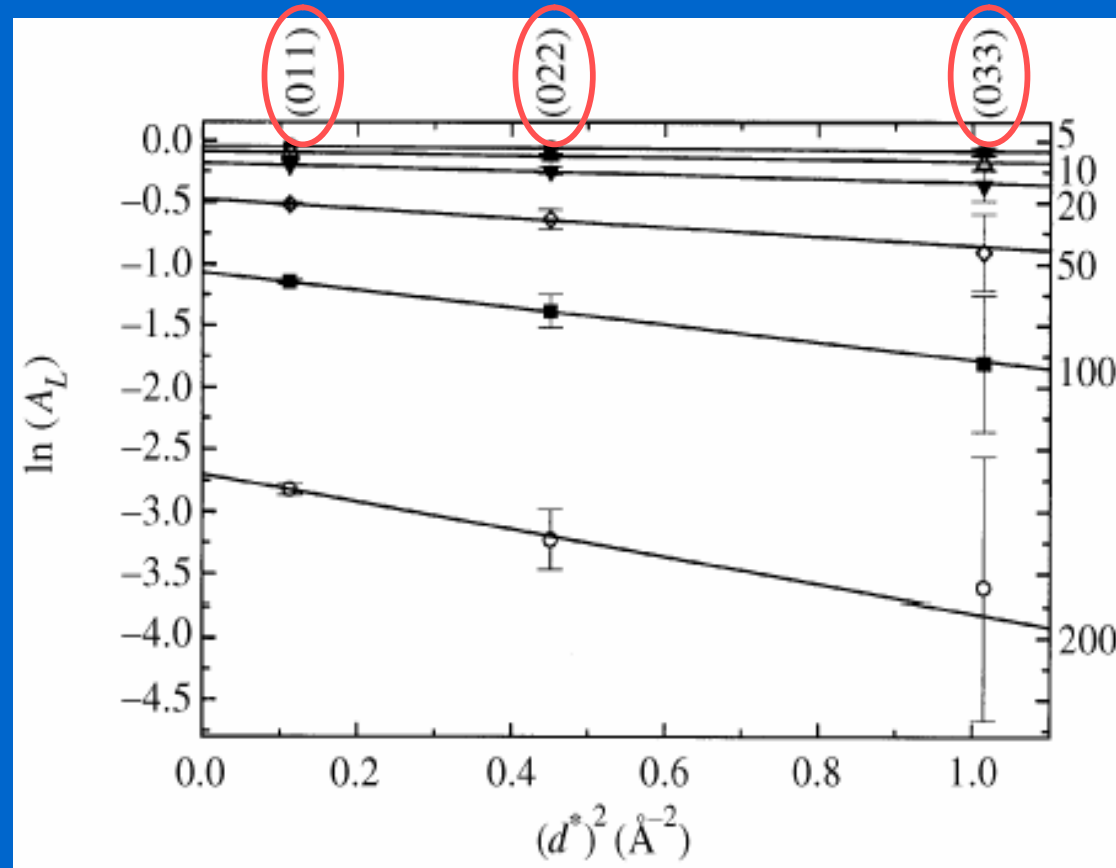
MARQX:



Y.H. Dong & P. Scardi, *J. Applied Crystallography* 33 (2000) 184-189.



PROFILE FITTING + WARREN-AVERBACH METHOD

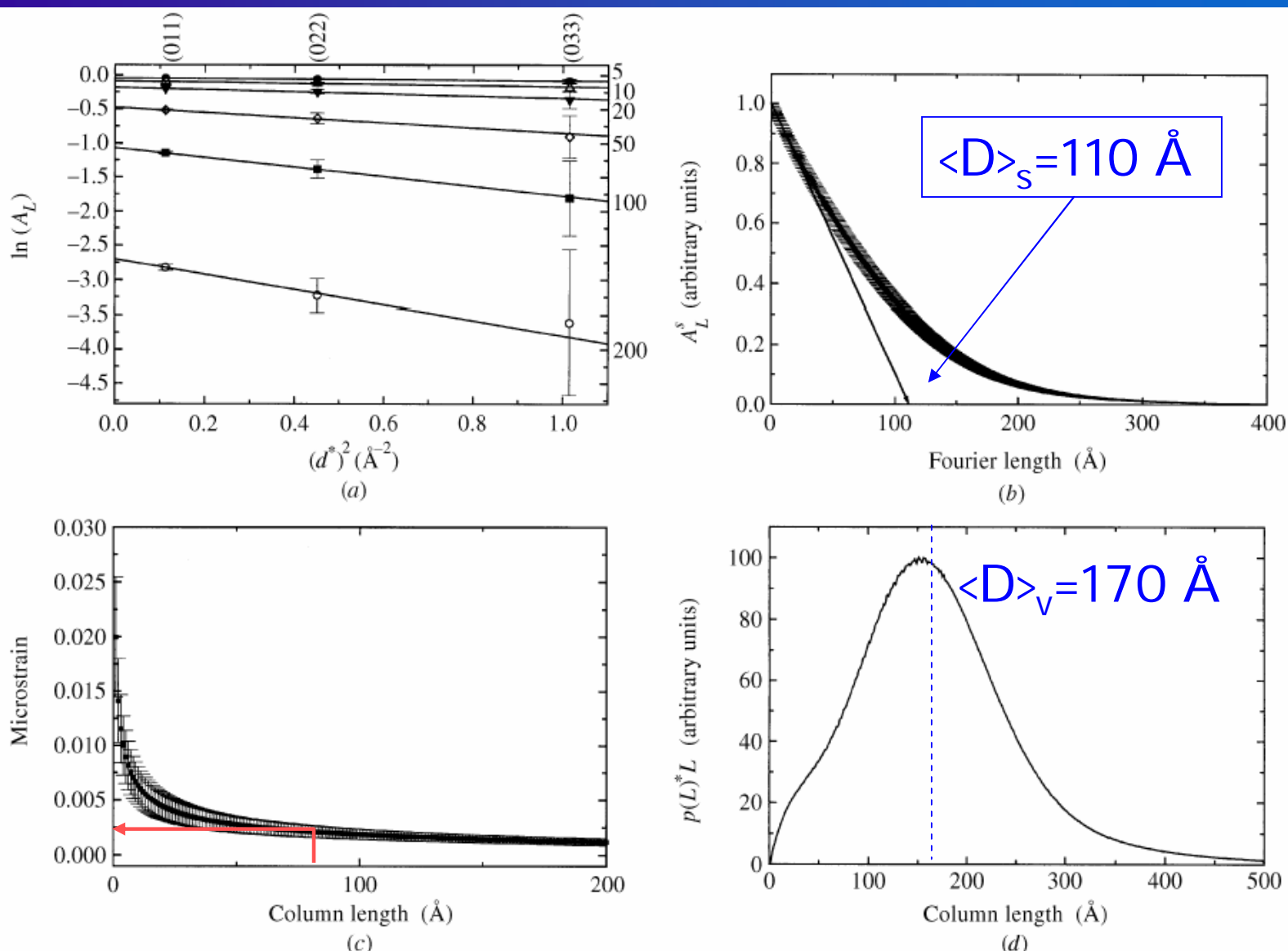


Warren-Averbach plot: intercepts \hat{a} A_L^S slopes \hat{a} $\langle e_{hkl}^2(L) \rangle$

Y.H. Dong & P. Scardi, *J. Applied Crystallography* 33 (2000) 184-189



PROFILE FITTING + WARREN-AVERBACH METHOD



Y.H. Dong & P. Scardi, *J. Applied Crystallography* 33 (2000) 184-189



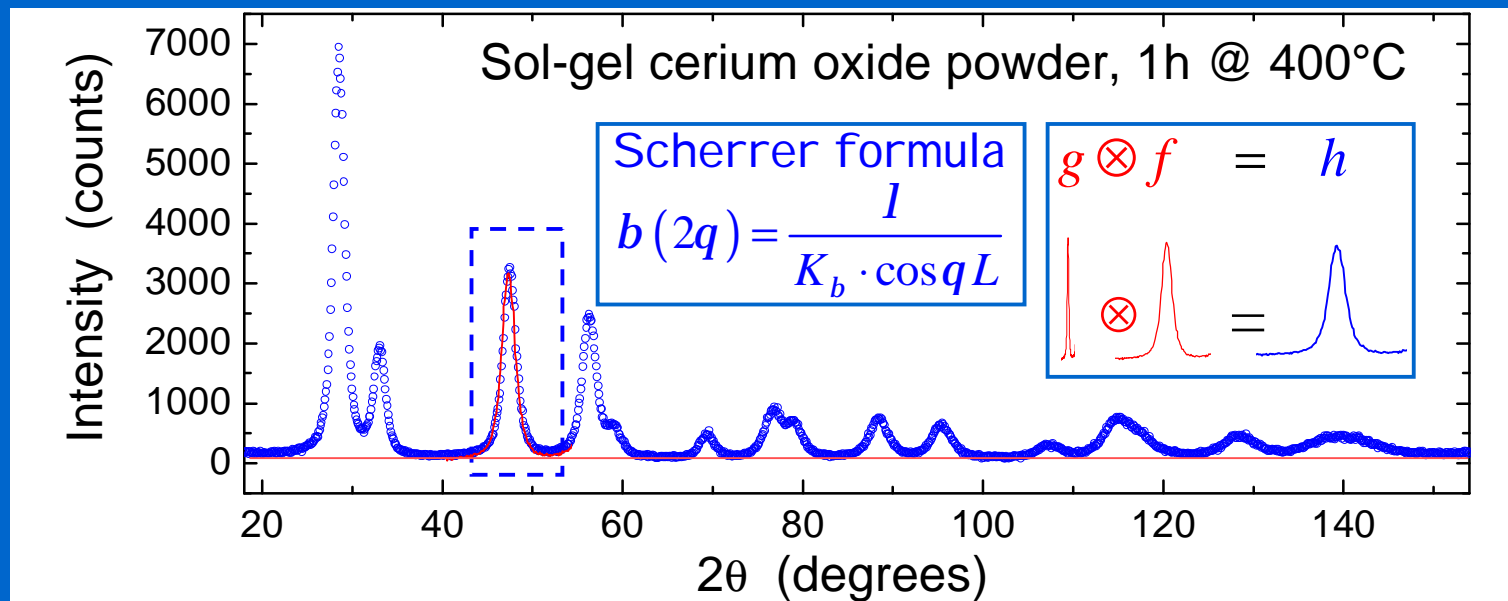
Advanced methods: Whole Powder Pattern Modelling (WPPM)



Traditional Line Profile Analysis

Most traditional methods are based on a multiple-step procedure:

1. Correction of line profiles for the instrumental component/backgr.
2. Extraction of line profile data (FWHM, β , Fourier coefficients, ...), typically by analytical profile fitting
3. Application of physical models to parameters *extracted* from the experimental pattern.

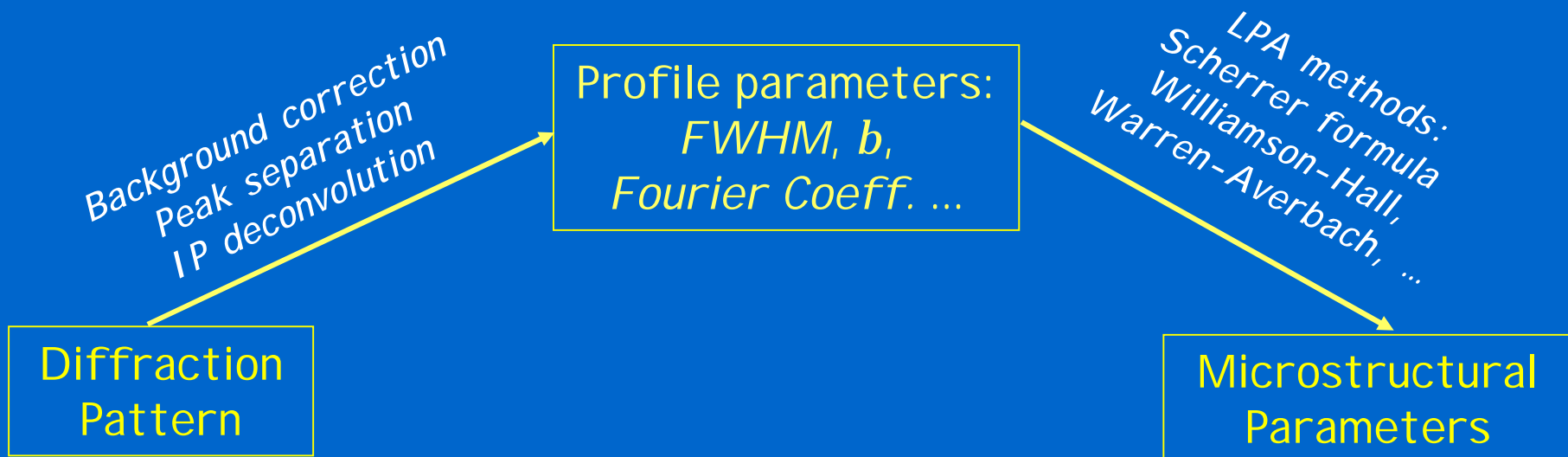




Traditional Line Profile Analysis

Most traditional methods are based on a multiple-step procedure:

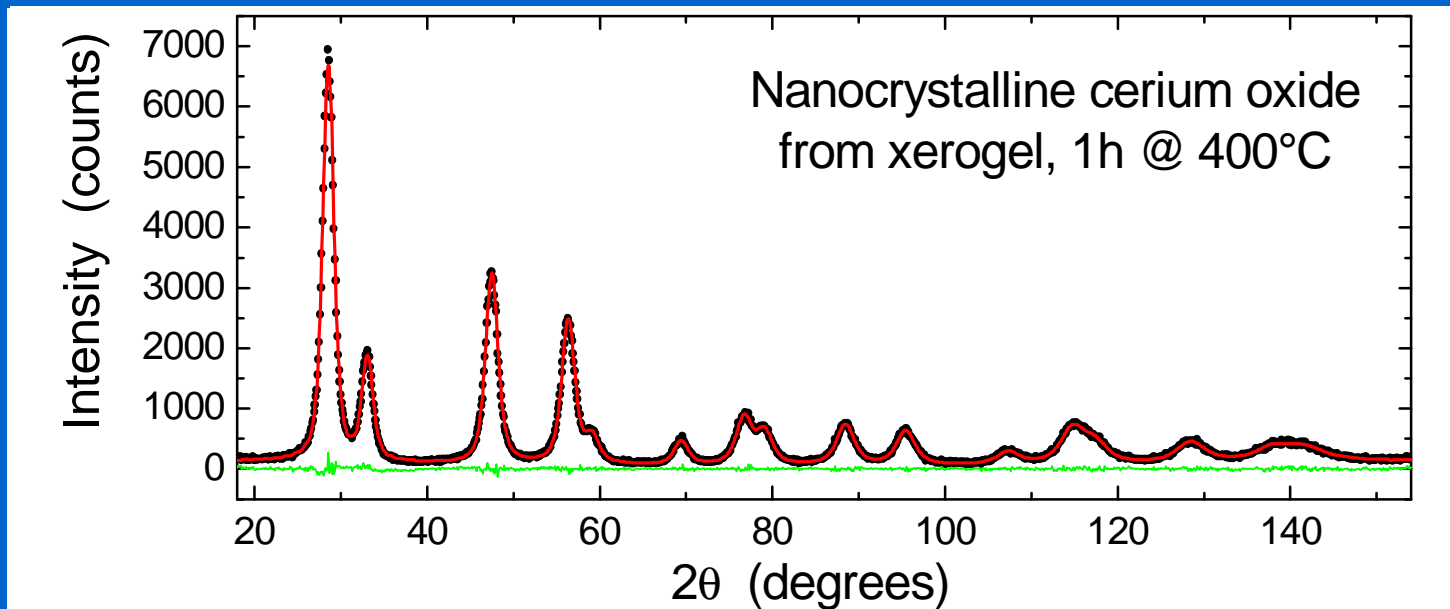
1. Correction of line profiles for the instrumental component/backgr.
2. Extraction of line profile data (FWHM, β , Fourier coefficients, ...), typically by analytical profile fitting
3. Application of physical models to parameters *extracted* from the experimental pattern.





Whole Powder Pattern Modelling

WPPM is based on a direct modelling of the experimental pattern, based on physical models of the microstructure and lattice defects:



M. Leoni, R. Di Maggio, S. Polizzi & P. Scardi, *J. Am. Ceram. Soc.* 87 (2004) 1133.



Diffraction line profile: a convolution of effects

The Whole Powder Pattern Modelling follows a Fourier analysis (like e.g. the Warren-Averbach method) but adopts a *convolutive approach*

$$I(d^*) = I^{IP}(d^*) \otimes I^S(d^*) \otimes I^D(d^*) \otimes I^F(d^*) \otimes I^{APB}(d^*) \otimes I^C(d^*) \otimes I^{GRS}(d^*) \dots$$

the Fourier Transform of $I(s)$ is the product of the FTs of the single profile components

$$I(d^*) \propto \int_{-\infty}^{\infty} \mathfrak{L}(L) e^{2\pi i L \cdot s_{hkl}} dL$$

$$\mathfrak{L} = \prod_i A_i = A^{IP} \cdot A^S \cdot A^D \cdot A^F \cdot A^{APB} \cdot \dots$$

Instrumental Profile

Dislocations

APB

Domain size

Faulting

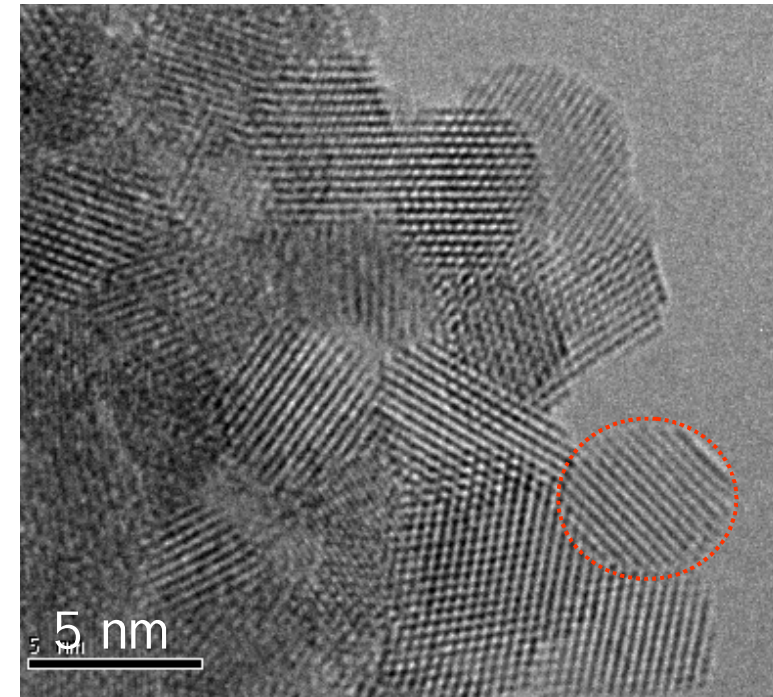
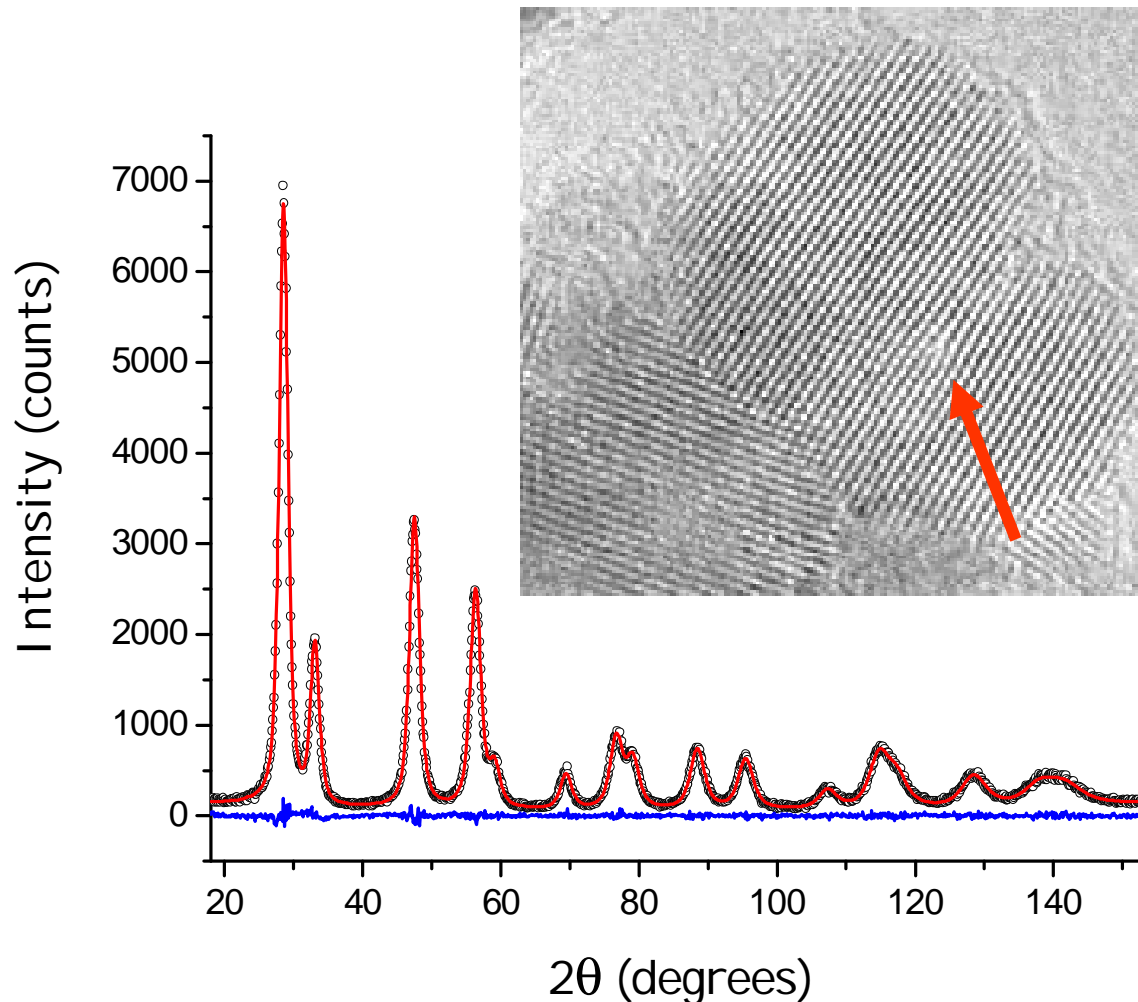


Whole Powder Pattern Modelling (WPPM) Applications



WPPM application: nanocrystalline Ceria

Nanocrystalline cerium oxide from sol-gel route

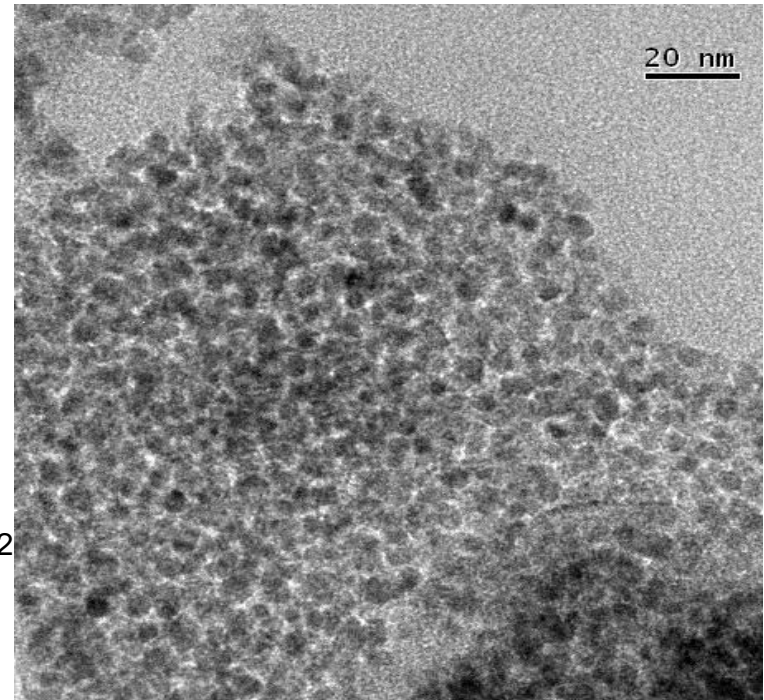
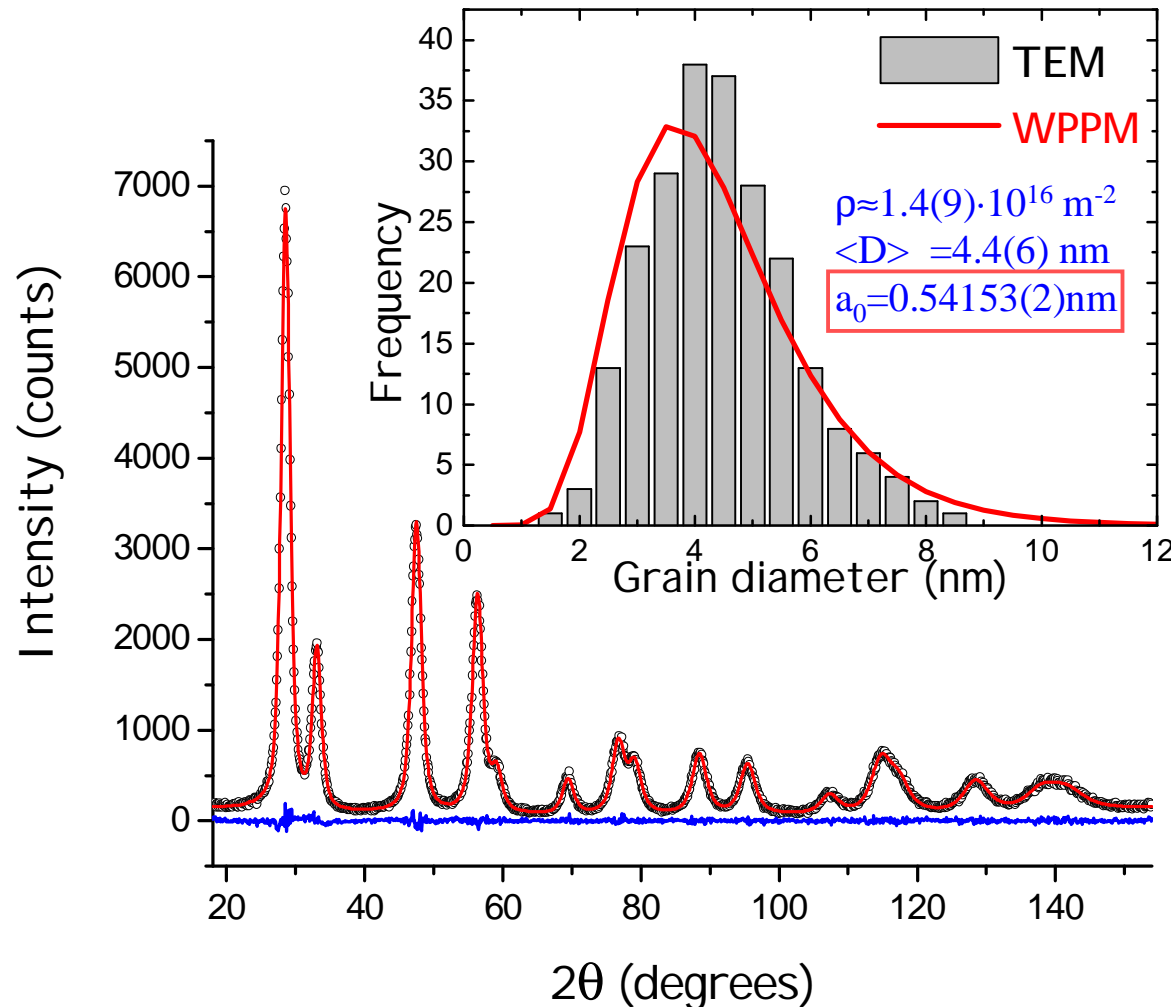


- P.Scardi, Z. Kristallogr 217 (2002)
- M. Leoni & P.Scardi, in *Diffraction Analysis of Materials Microstructure*. E.J. Mittemeijer & P. Scardi, editors. Berlin: Springer-Verlag. 2004



WPPM application: nanocrystalline Ceria

Nanocrystalline cerium oxide from sol-gel route



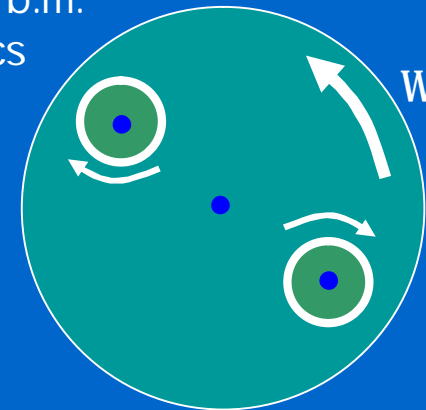
- P. Scardi, *Z. Kristallogr* 217 (2002)
- M. Leoni & P. Scardi, in *Diffraction Analysis of Materials Microstructure*. E.J. Mittemeijer & P. Scardi, editors. Berlin: Springer-Verlag. 2004



Planetary ball milling



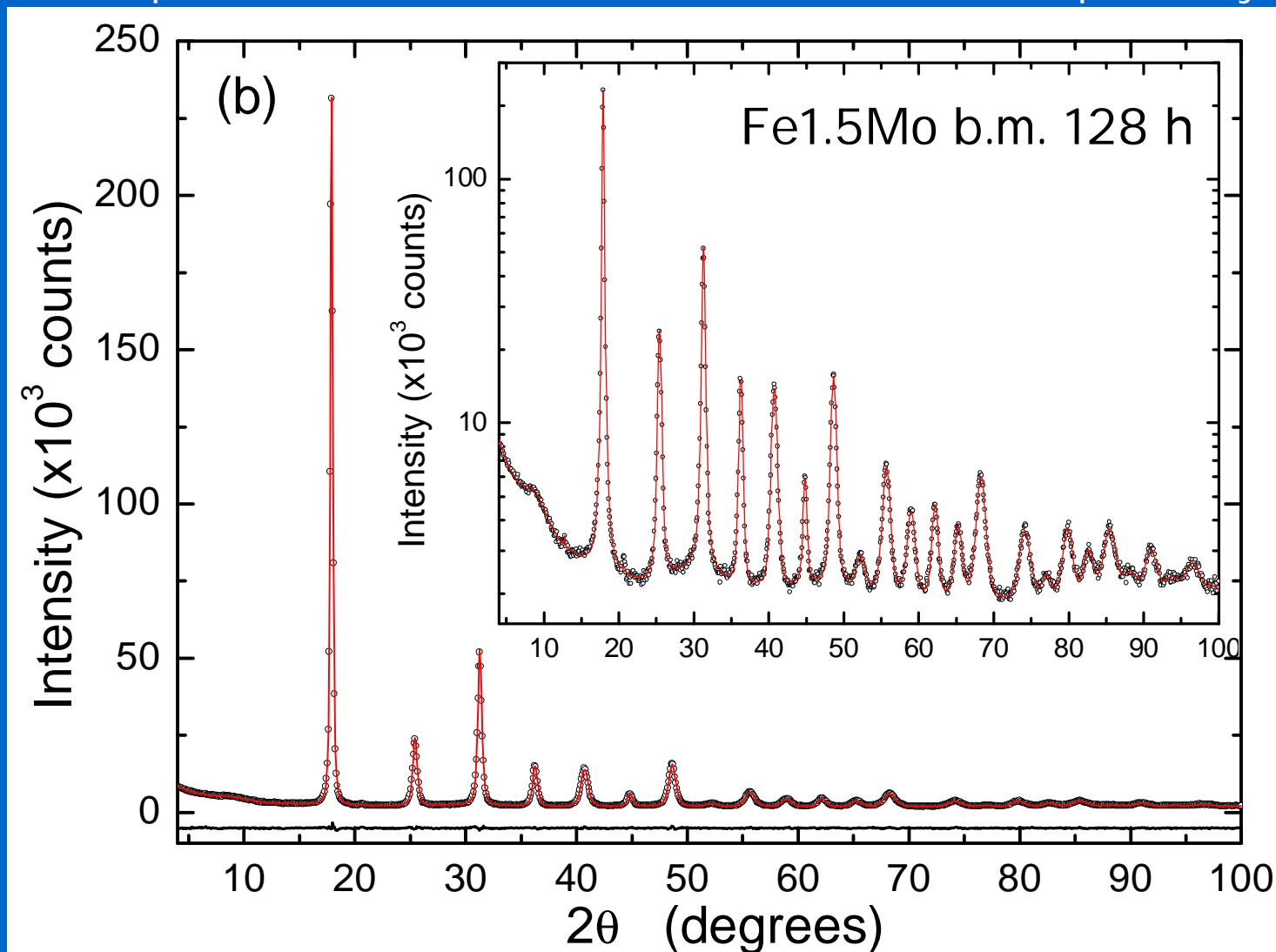
Planetary b.m.
schematics





SR XRD - ball milled Fe 1.5Mo

Fe1.5Mo powder ball-milled for *96 hours* in a Fritsch P4 planetary mill

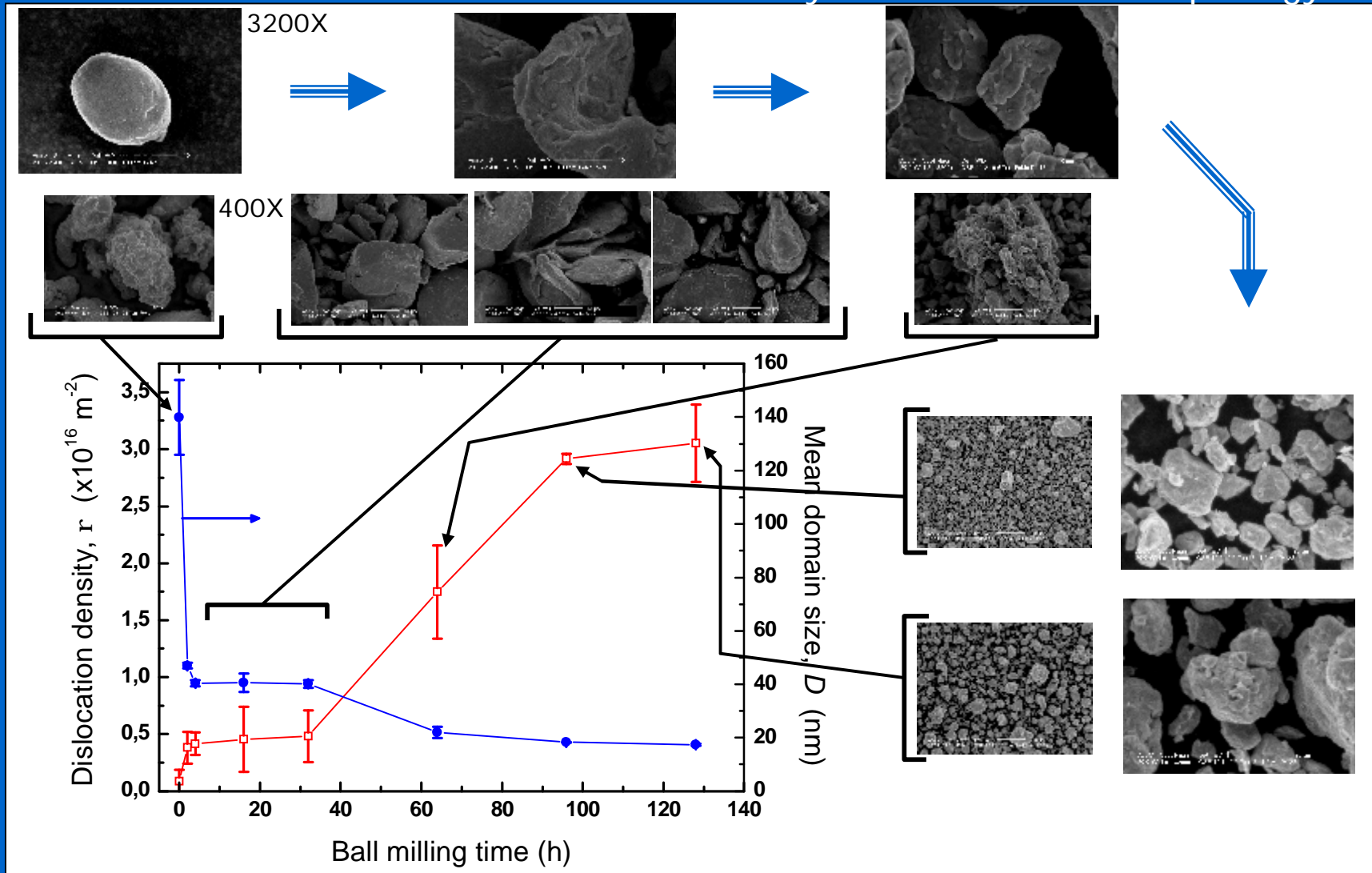


P. Scardi in "Powder Diffraction. Theory and practice". Eds: R. E. Dinnebier & S. Billinge. The Royal Society of Chemistry, 2006. In press.



SR XRD - ball milled Fe 1.5Mo

Ball-milled Fe_{1.5}Mo: dislocation density/domain size vs. morphology

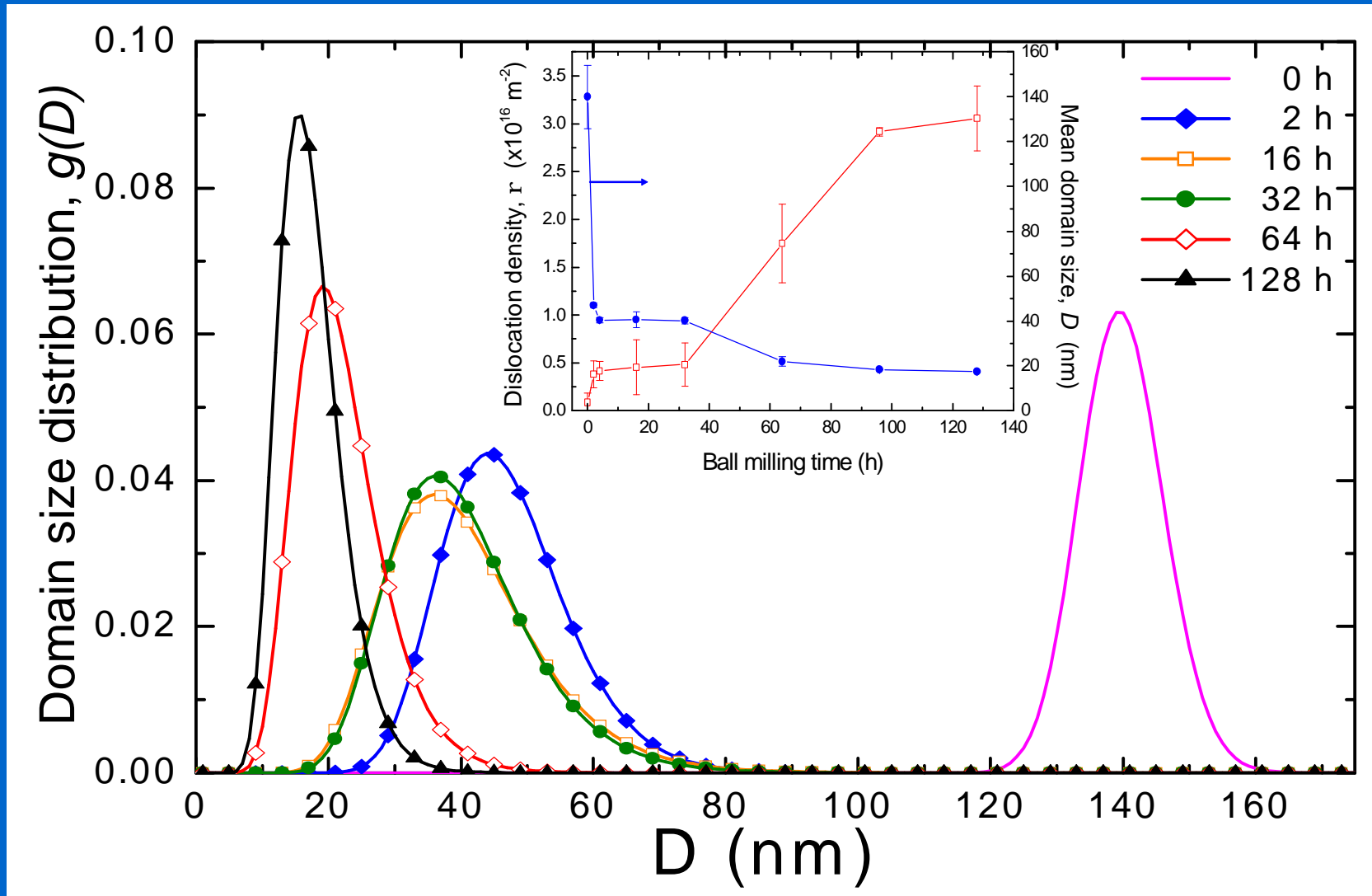


P. Scardi in "Powder Diffraction. Theory and practice". Eds: R. E. Dinnebier & S. Billinge. The Royal Society of Chemistry, 2006. In press.



SR XRD - ball milled Fe 1.5Mo

In addition to mean sizes, WPPM provides the distributions:

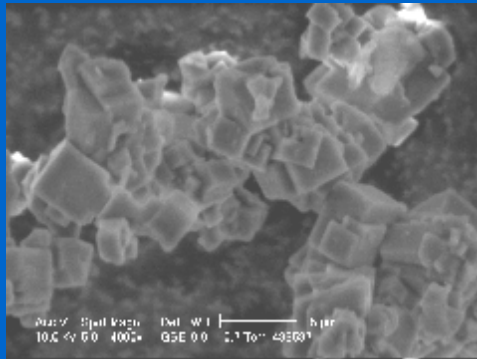


P. Scardi in "Powder Diffraction. Theory and practice". Eds: R. E. Dinnebier & S. Billinge. The Royal Society of Chemistry, 2006. In press.

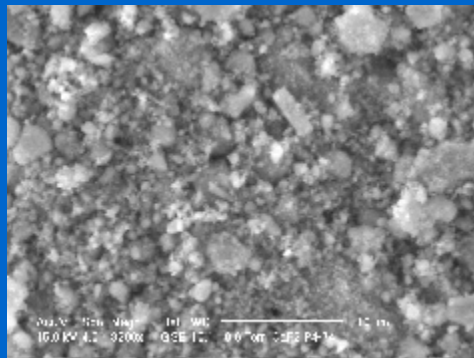


ball milled Fluorite

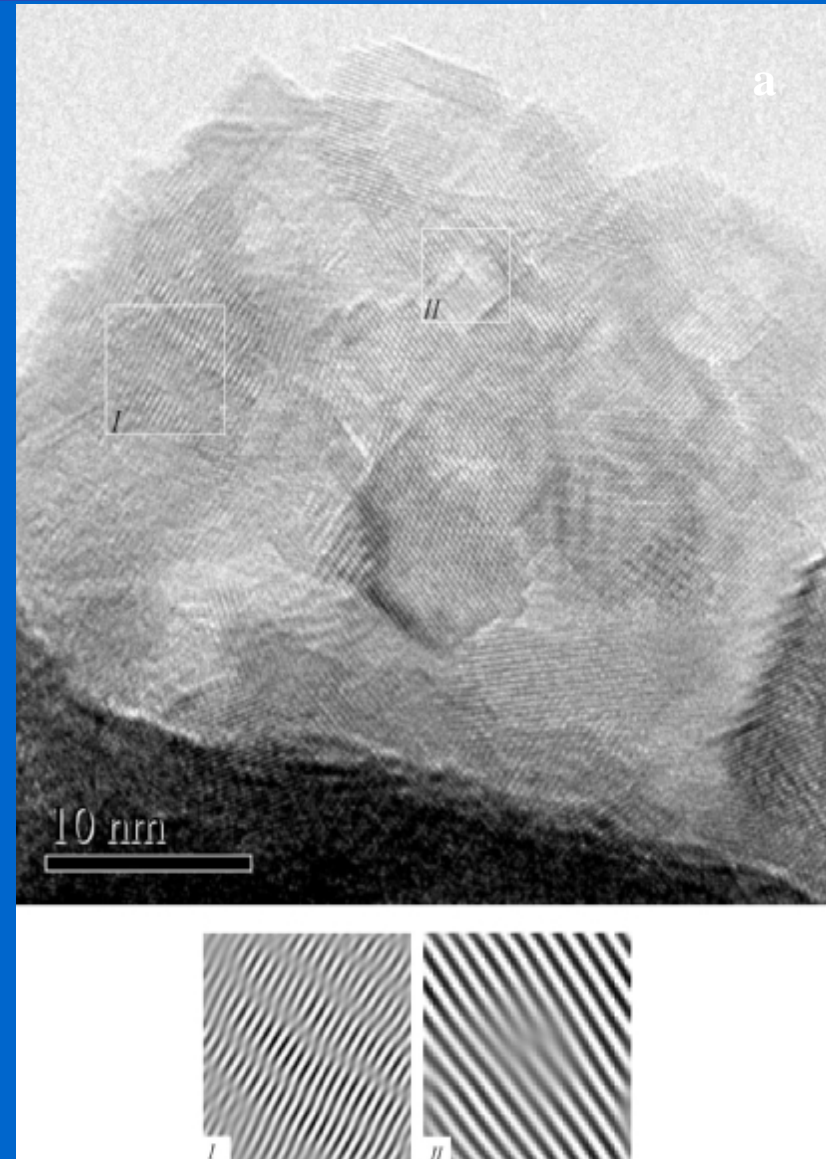
Effect of domain size and defectivity on the solubility of fluorite (ionic product)



0 h b.m.



32 h b.m.

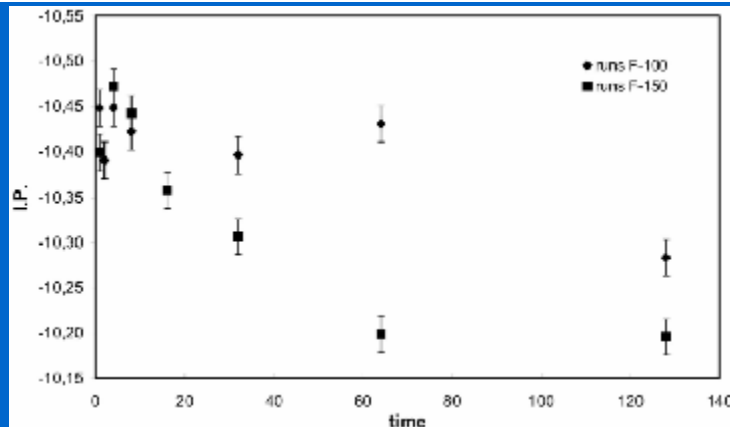
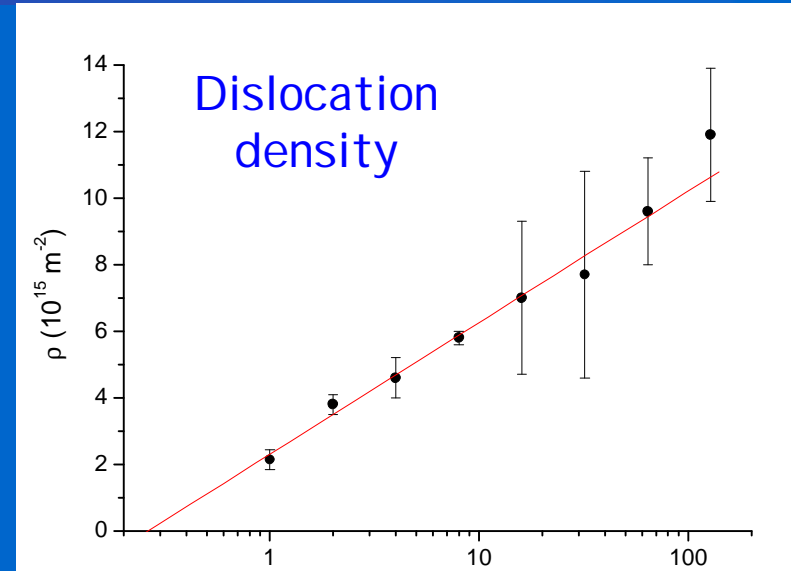
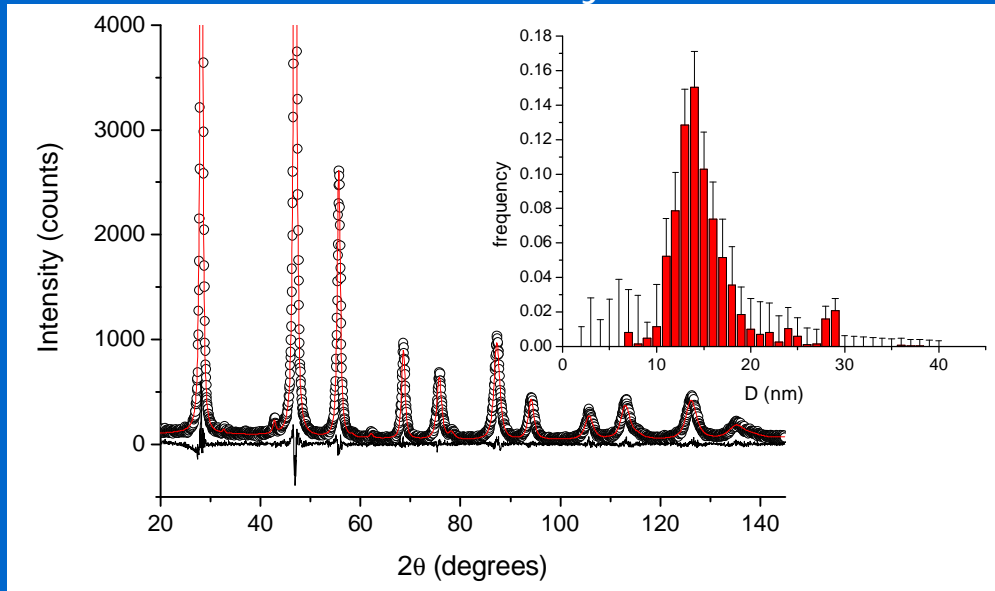


G. De Giudici et al. *Geochim. Cosmochim. Acta* 29 (2005) 4073



ball milled Fluorite

Effect of defectivity on the Ionic Product in near-stationary conditions

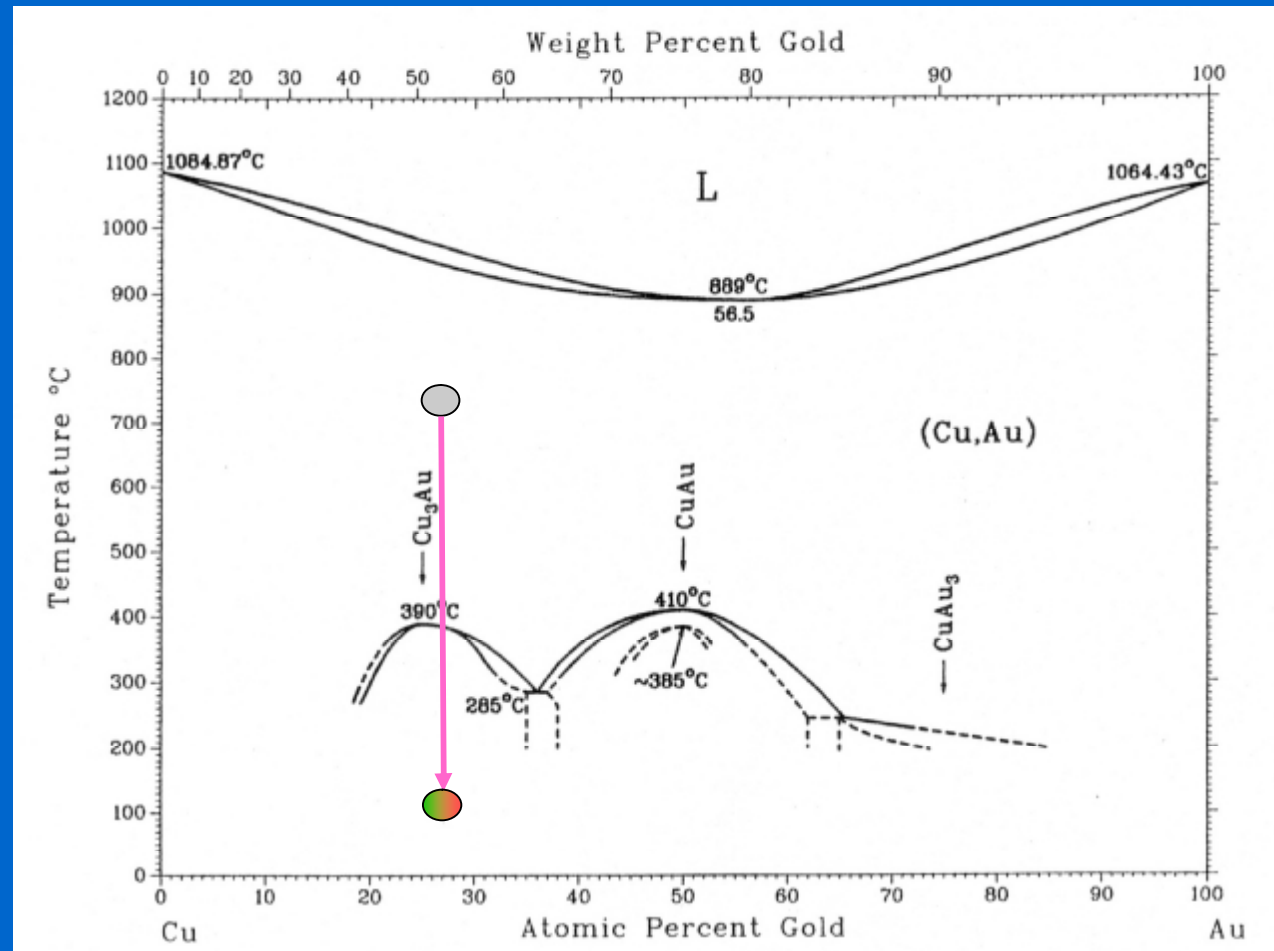
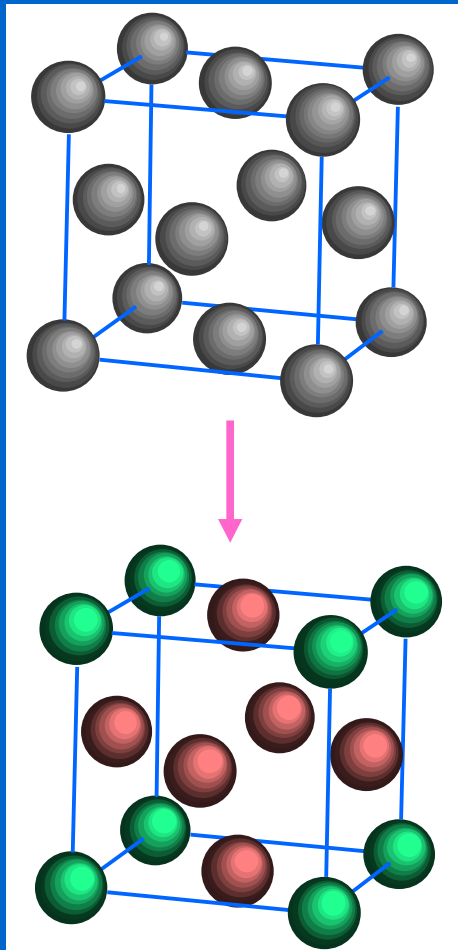


G. De Giudici et al. *Geochim. Cosmochim. Acta* 29 (2005) 4073



APDs in Cu_3Au

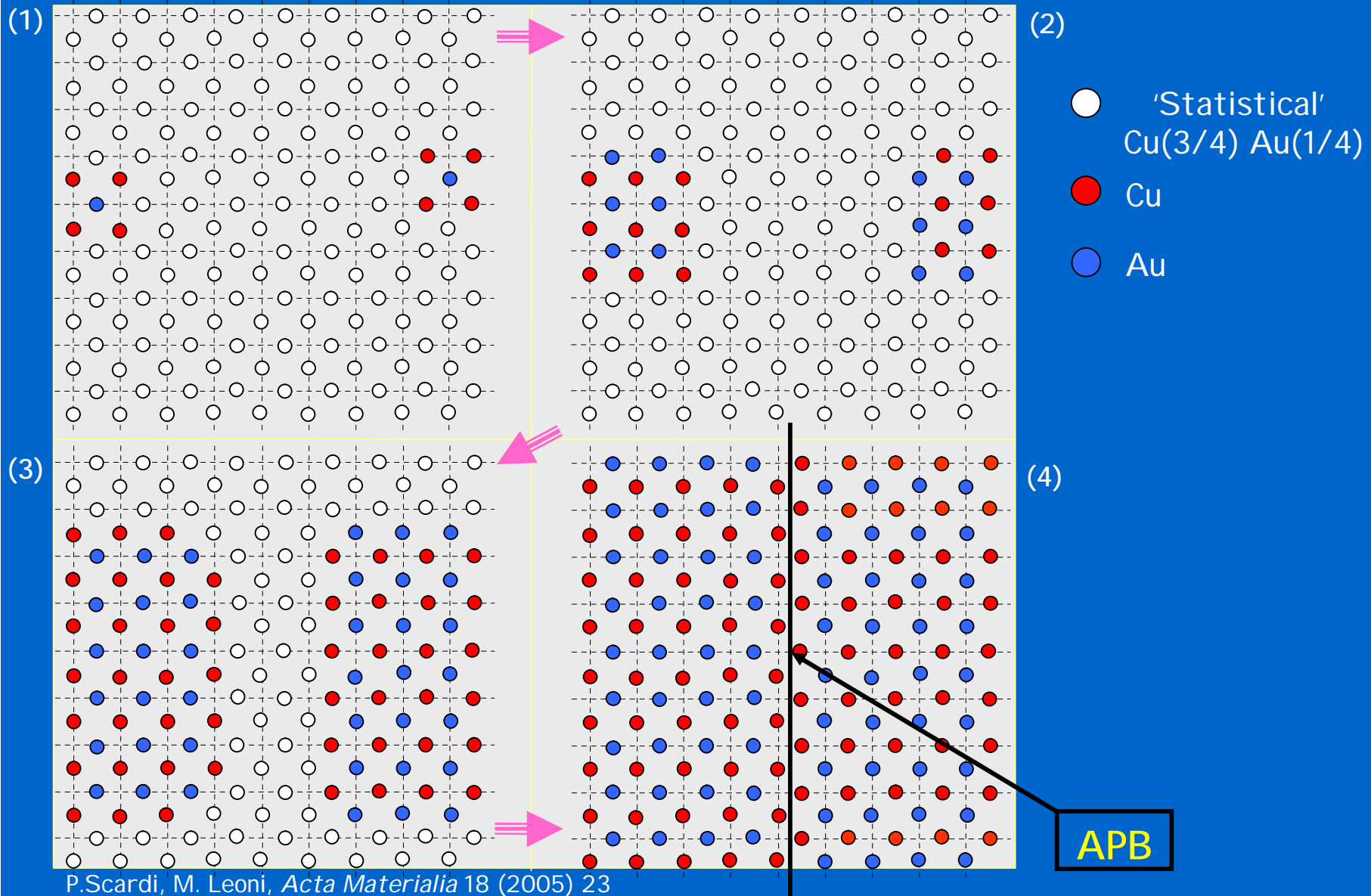
Anti Phase Domains form during the ordering process in Cu_3Au . The o/d process can be thermally activated



P.Scardi, M. Leoni, *Acta Materialia* 18 (2005) 23



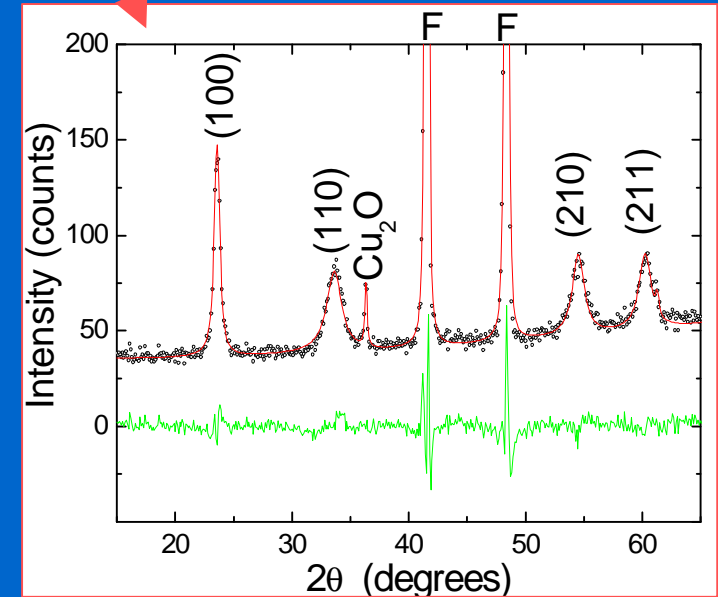
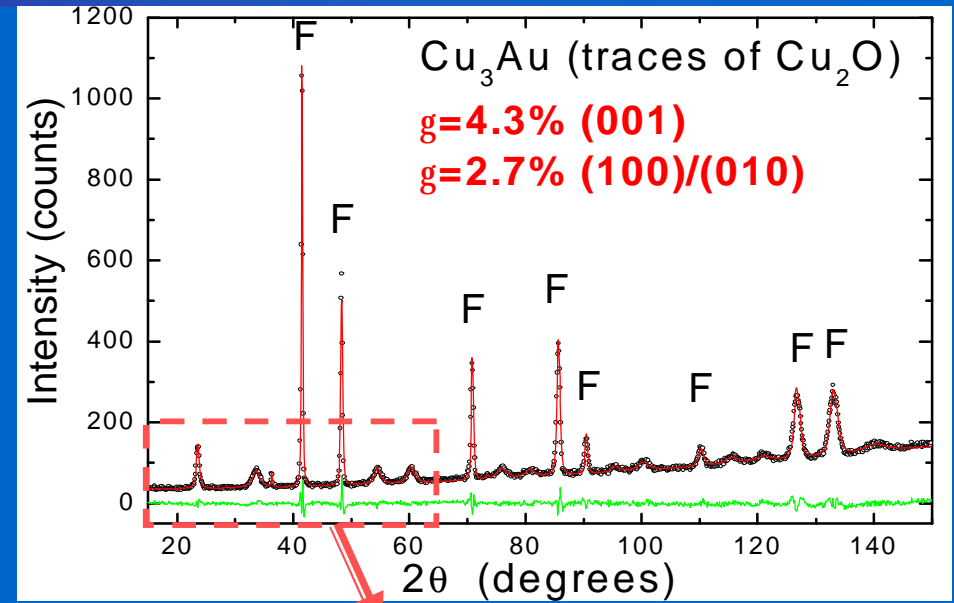
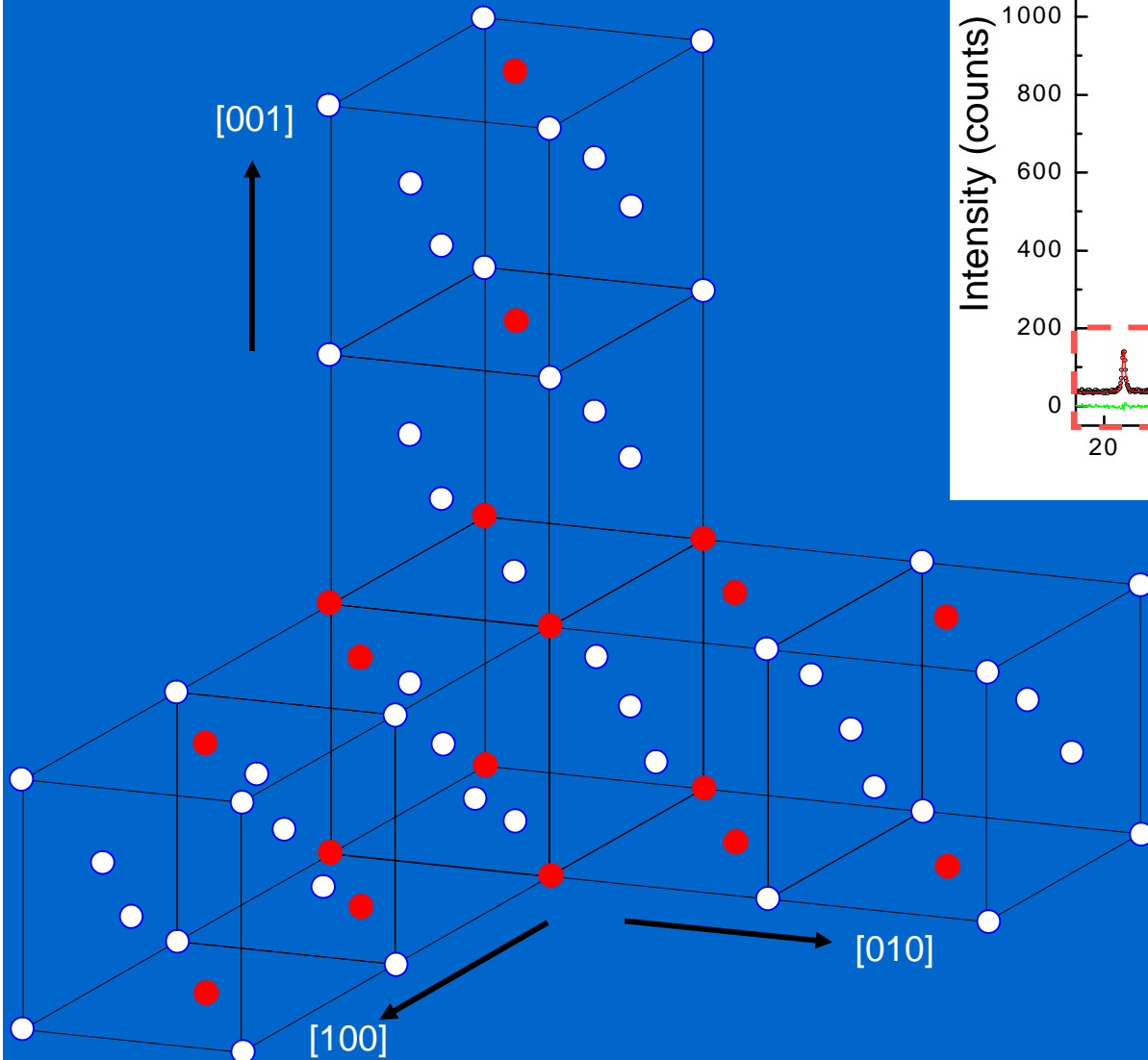
APDs in Cu_3Au





APDs in Cu_3Au

P.Scardi, M. Leoni, *Acta Materialia* 18 (2005) 23





General references

B.E. Warren, *X-ray Diffraction*, Addison-Wesley, Reading, MA, 1969.

A. Guinier, *X-ray Diffraction*, Freeman & Co, S. Francisco, 1963.

A.J.C. Wilson, *X-ray Optics*, 2nd ed., Methuen & Co, London, 1962.

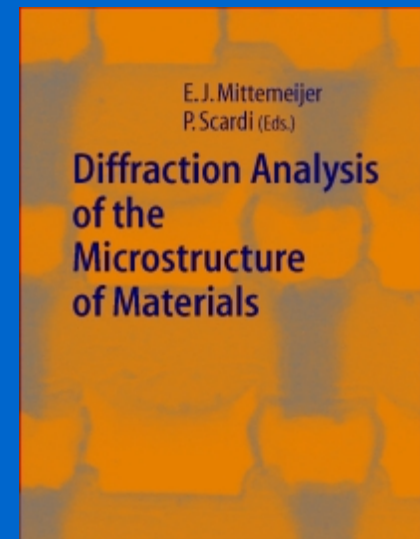
H.P. Klug & L.E. Alexander, *X-ray Diffraction procedures*, Wiley, New York, 1974.

B.D. Cullity, *Elements of X-ray Diffraction*, Addison-Wesley, Reading Ma, 1978.

Diffraction Analysis of Materials Microstructure

E.J. Mittemeijer & P. Scardi, editors.

Berlin: Springer-Verlag, 2003.





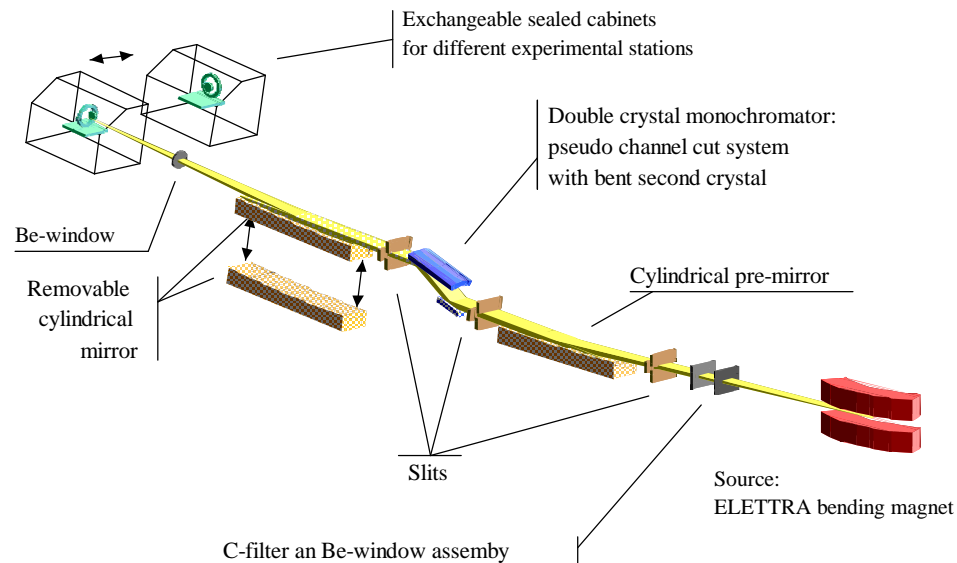
WPPM: references

- P.Scardi & M. Leoni, *Acta Cryst. A* 57 (2001) 604
- P.Scardi & M. Leoni, *Acta Cryst. A* 58 (2002) 190
- P.Scardi, *Z. Kristallogr.* 217 (2002) 420
- P.Scardi, M. Leoni, R. Delhez *J. Appl. Cryst.* 37 (2004) 381
- M. Leoni, P. Scardi *J. Appl. Cryst.* 37 (2004) 629
- P.Scardi, M. Leoni, *Acta Materialia* 18 (2005) 23
- P.Scardi & M. Leoni, *J. Appl. Cryst.* 39 (2006) 100

Software MarqX, PM2K:
Paolo.Scardi@unitn.it
Matteo.Leoni@unitn.it



MCX - A new beamline for Materials Characterization by XRD at ELETTRA (Trieste, Italy) A. Lausi (Sincrotrone Trieste), P. Scardi (Univ. Trento & INSTM)



Under construction à end 2006



Examples of typical applications

- Residual stress and texture analysis in thin films by multiple wavelength XRD
- Surface analysis by grazing incidence XRD and reflectivity
- Medium-low energy (3.5÷20 keV) anomalous scattering XRD
- Line Profile Analysis (e.g., nanocrystalline, highly defected materials)
- Non-ambient studies (controlled atmosphere, high temperature kinetics)
- Surface mapping by microdiffraction (diffraction on small area)